TÉCNICO LISBOA

A simple MILP optimization model for the economic assessment of a solar photo-voltaic system to feed a university campus and a set of surrounding residential complexes

Stefano Casarin

Thesis to obtain the Master of Science Degree in

Mechanical Engineering

Supervisors: Prof. Andrea Lazzaretto
Prof. Carlos Augusto Santos Silva

Examination Committee

Chairperson: Prof. Edgar Caetano Fernandes
Supervisor: Prof. Carlos Augusto Santos Silva
Member of the Committee: Prof. Susana Margarida da Silva Vieira

November 2018

To my family.

Acknowledgments

First and foremost I would like to express my very great appreciation to professors Carlos Santos Silva and Andrea Lazzaretto, my research supervisors, for their patient guidance, enthusiastic encouragement and useful critiques of this research work.

I would also like to thank Dr. Sergio Rech and Prof. Filipe Mendes for their advice and assistance in system and solar energy modeling, respectively.

My grateful thanks are also extended to the T.I.M.E. association that made this double degree exchange possible.

Special thanks to my my parents in particular, and to all my family for their support and encouragement throughout all my studies.

I wish to thank my flatmates who have endured the last weeks as much as myself, especially Francisco, whose computer was fundamental for the conclusion of this work, Miguel for his translation support, and Rita for her help with the graphics.

Finally, I thank from the bottom of my heart all of the people whose path has crossed with mine and have left a permanent mark on me. You know who you are, and a part of this success is also yours.

Resumo

O Instituto Superior Técnico (IST) tem um campus no centro de Lisboa e o seu consumo de energia elétrica constitui uma parte substancial do orçamento anual. Rodeado por muitos complexos residenciais com área de telhado disponível, há um elevado potencial para a produção de energia solar. O objetivo deste trabalho é encontrar a configuração ótima, isto é, o número e o tipo de equipamentos, que o IST teria que instalar nos telhados dos edifícios circundantes para que tanto o campus como os residentes pudessem reduzir os custos anuais relativos à energia elétrica. Um modelo MILP é construido de forma a encontrar a configuração ótima do sistema: o campus é caracterizado por uma curva de consumo elétrico e duas tecnologias: módulos photo-voltaicos (PV) e coletores solares térmicos (ST) com armazenamento térmico; quatro edifícios são considerados, cada um caracterizado pela sua área de superfície disponível e o seu perfil de consumo elétrico e térmico. O modelo foi implementado durante quatro dias típicos, cada um representando uma época do ano. Os resultados mostram que os requisitos de energia térmica de uma habitação não são suficientemente significativos para justificar um investimento em ST. No cenário de base, toda a área disponível é utilizada para implementar módulos PV Finalmente, a análise da sensibilidade nos custos unitários dos módulos PV mostra que a poupança do IST decresce fortemente com o aumento do custo, enquanto que a dos residentes permanece constante até o custo ser de tal forma alto que não permita o uso total da superfície.

Palavras-chave: MILP, otimização, energias renováveis, energia solar, energia solar foto-voltaica, geração distribuída.

Abstract

The Instituto Superior Técnico (IST) university has a campus located in the center of Lisbon and its electrical consumption represent a relevant share of the yearly budget. Being surrounded by plenty of residential complexes with available roof surface, there is a high potential for solar energy production. The goal of this work is to find an optimal configuration, i.e. the number and type of equipment, that IST should install on the roofs of the surrounding buildings so that both the campus and the residents can reduce their yearly electrical energy related costs. A MILP model is built to find the optimal configuration of the system: the campus is characterized by an electric consumption curve and two technologies – photo-voltaic modules (PV) and solar-thermal collectors (ST) with thermal storage; four buildings are considered, each one characterized by an amount of available surface and an electric and a thermal load consumption profiles. The model has been run over four days, each representative of one season. Results show that the households' thermal energy requirements are not significant enough to justify an investment in ST. In the base scenario all of the available surfaces are filled with PV modules. Finally a sensitivity analysis on the PV modules' unitary cost shows that IST savings strongly decrease with the increase of this cost, while the residents' are affected only as if the specific cost is high enough not to cover completely the available surfaces.

Keywords: MILP, optimization, renewable energy, solar energy, photo-voltaic, distributed generation

Contents

List of Tables

List of Figures

Nomenclature

Greek symbols

α	optic absobitiviy coefficient
β	surface's slope, deg
δ	solar declination, deg
η	efficiency
γ	azimuth angle of a surface, deg
γ	solar hour angle, deg
ϕ	latitude, deg
ρ	density, $\mathrm{kg\,m^{-3}}$
ρ_g	gound reflection constant
τ	optic transmissivity coefficient
θ	incidence angle, deg

Roman symbols

AFA	available floor area, $\mathrm{m^2}$
C, c	total and specific costs, €
c_p	specific heat, $\mathrm{J\,kg^{-1}\,K^{-1}}$
DH	degree-hours, °C
$f(\mathbf{x}(t))$	objective function
F_R	heat removal factor
G	solar radiation, $\mathrm{W\,m^{-2}}$
$g(\mathbf{x}(t))$	equality constraint
G_{sc}	solar constant, $\mathrm{J\,m^{-2}}$
GAP	glazing area percentage, $\%$
h	height, m
$h(\mathbf{x}(t))$	inequality constraint
I	solar irradiation, $\mathrm{J\,m^{-2}}$
i	interest rate, $\%$
k	constant of proportionality
L	heating loss coefficient, $\mathrm{kW\,K^{-1}}$
Lat	latitude, deg
LVL	amount of stored energy, kWh
M	constant parameter used for the "big-M" linearization
N	number of elements
n	expected lifetime, year
P	electric energy, kWh
Q	thermal energy, kWh
r_t	cost actualization factor
Rev	revenues, €
S	surface, $\mathrm{m^2}$
T	temperature, °C
t	time, h
U	thermal transmittance, $\mathrm{W\,m^{-2}\,K^{-1}}$
V	volume, $\mathrm{m^3}$

Subscripts and superscripts

0	extraterrestrial
b	beam
c	cold
ch	charge
$coll$	ST collector
d	diffuse
dd	design day
dhw	domestic hot water
$disch$	discharge
$diss$	dissipated
eh	electric heater
el	electric
f	fluid
h	hot
inv	investment
ist	campus
m	mean
max	maximum
mod	PV module
n	normal
$O\&M$	operation and maintenance
pv	photo-voltaic
ref	reference
sc	surface sunset time
sh	space heating
sr	sunrise
ss	sunset
st	solar thermal
T	total
th	thermal
ts	thermal storage
usr	residential complex
z	zenith

Glossary

CCHP Combined cool, heat, and power.

CHP Combined heat and power.

DER Distributed energy resources.

DG Distributed generation.

DHW Domestic hot water.

EE Electric energy.

EH Energy hub.

EU European Union.

GHG Greenhouse gases.

IST Instituto Superior Técnico.

MILP Mixed Integer Linear Programming.

MIP Mixed Integer Programming.

NG Natural gas.

PV Photo-voltaic.

RES Renewable energ sources.

SH Space heating.

ST Solar thermal.

TS Thermal storage.

USR Residential building composed by multiple apartments..

Wp Watt-peak.

Chapter 1

Introduction

The "2020 climate & energy package" is a set of policies, at the European Union level, that sets three targets to be met by 2020 [1]:

- 20 % cut in greenhouse gas () emissions (from 1990 levels);
- 20 % of energy generated from renewable energy sources (RES);
- 20 % of improvement in energy efficiency.

This set of objectives is one of the milestones set for the long-term goal of reducing the GHG emissions by 80 to 90 % by 2050 [2]. By 2050 about two thirds of the world population will be living in cities while it has been estimated that European cities are accountable for the consumption of about 80 % of the overall EU energy and at the same time are responsible for about the same share of GHG [3, 4]. The efforts to improve the GHG emissions shall therefore be focused on urban contexts.

As of 2015 Portugal – among other member states – is considered on track for the achievement of the 2020 targets [5]. In recent years a number of policies have been implemented to promote energy efficiency: the first regulation for the energy performance of residential buildings dates back to 1990 and has been outdated in 2006 by the *Regulamento das Características de Comportamento Térmico dos Edifícios* (RCCTE), receiving the 2002/91/CE EU directive [6]. The latest regulation is from 2013 and the *Regulamento de Desempenho Energético dos Edifícios de Habitação* (REH) [7].

Instituto Superior Técnico (IST) is one of the most prominent academic institution in Portugal and boasts several partnerships with renowned universities all over the world, together with a prolific academic research activity. It has three campuses, the main one being the Alameda campus, situated in the center of Lisbon.

The Alameda campus was situated in the outskirts of Lisbon, but with the city's expansion in the first half of the XX century, it quickly became surrounded by multi-apartment buildings. The IST works all year long, with the exception of two weeks of the month of August, and requires a high amount of energy for didactic, administrative, and research activities. An internal energy audit revealed that the energy mix is composed for 81 % of electrical energy (EE), while 19 % is natural gas (NG). The energy consumption

represents a relevant share of the yearly budget, and to this date it only relies on the connection to the electric grid and NG distribution network. The campus does not perform any self generation.

A way to reduce the energy-related costs and decrease the respective carbon footprint would be the integration of RES generators.

Portugal is a country with an abundant availability of RES: in 2016 alone the gross wind electric generation was 12 474 GWh [8], while the yearly sum of global irradiation collected with an optimally sloped surface is estimated greater than 2000 kWh m^{-2} [9].

Due to the location in which the campus is situated, wind energy generators can not possibly be installed in an urban area. On the other hand, solar energy is a much more viable option: the campus is surrounded by residential buildings, whose roofs are not yet equipped with neither solar photo-voltaic (PV) or thermal (ST) collectors: the produced energy therefore could be conveyed in low voltage thanks to the short distances.

The aim of this work is to assess the feasibility of a distributed generation (DG) network providing energy to IST campus and to those multi-apartment buildings that will host the energy conversion equipment, through a microgrid.

In different contexts DG has been proved a sustainable solution, being capable to provide higher quality of energy services and allowing the operation of systems according to the variable costs of EE, NG and other commodities [10].

1.1 State of the art

The concept of *Energy Hub* (EH) can be defined as “an interface between consumers, producers, storage devices in different ways: directly or via conversion equipment, handling one or several carriers” [11]. Under this perspective, IST campus has the potential to become an EH thanks to a careful design of the generators and their schedules.

Several approaches and optimization techniques have successfully been applied in both the design and the schedule operation of EH, polygeneration systems, distributed generation and microgrids [10–13]. The successful integration of energy from decentralized intermittent sources depends heavily on the optimisation of the energy systems [14].

Sigarchian et al. developed a model to find the optimal operating schedule of a polygeneration system using particle swarm optimization [15]. Fetanat and Khorasaninejad have used an ant colony optimization algorithm to design an hybrid PV-wind energy system, comparing it with other optimization methods [16]. The optimal size of heat storage devices as well as the operation of several power plant units is found by Christidis et al. through Mixed Integer Programming (MIP) [17]. Similarly Rech and Lazzaretto have used a mean integer linear programming (MILP) to find the optimal operating schedule of RES converters and the size of the energy storage devices of a small municipality [18]. The design and schedule plan of a complex distributed energy system (DER) assessing economic, environmental, and energetic aspects of the optimal combination of technologies and schedules is found with a MILP model by Ren and Gao [19]. Costa and Fichera developed a MILP model to obtain the optimal design and yearly schedule of

a combined heat and power (CHP) system serving an hospital facility under two scenarios: with and without thermal storage (TS) [20]. Ameri and Besharati developed a MILP model for the optimal design and operation of both the energy movers and the distribution network of a combined cool, heat, and power (CCHP) plant in Tehran [21].

In this work a MILP model has been developed to design a decentralized energy production network relying on solar energy. MILP has been chosen because such models have the advantage that – when convergence is attained – it is proven for the feasible solution to be optimal or close to optimal [22]. MILP is also being extensively used on energy hub models for being fast and reliable [23].

In the literature there are several softwares and languages to perform such analysis. Distributed Energy Resources - Customer Adoption Model (DER-CAM) is a powerful tool developed by the Berkeley Lab. It formulates problems as a MILP and finds globally optimal solutions for distributed energy resources investments, for either buildings or multi-energy microgrids [24]. This tool has been thoroughly used to find the optimal design and configurations of DER systems [25–27].

There are other tools to model and solve complex optimization problems: General Algebraic Modeling System (GAMS) is a modeling system for mathematical programming and optimization, is suitable for the modeling of several types of problems and supports a large variety of solvers [28]. Other suitable languages to develop DER models (among others) are: C, C++, Java®, Python®, Matlab®. The most used solvers for MIP, MILP, and other non-linear problems are CPLEX® and GUROBI® [29, 30].

1.2 Objectives

The aim of this work is to assess the economic feasibility of the implementation of a decentralized renewable energy system. This translates into the search for the optimal configuration of the energy generation system i.e. the amount of installed PV modules, ST collectors, and the size of the TS tank (if any) that will produce a reduction of the energy-related expenses for both the campus and the residential complexes.

If the conditions are favorable, IST and the owners of the apartments to which the rooftops belong will form a synergistic cooperative: the former will get the PV energy that is not self-consumed, while the latter receive free renewable energy by making available the unused roof surface.

The reason for considering the ST technology is that in Portugal it is common to use EE for heating purposes: a ST system would reduce the renewable PV energy self-consumption allowing more EE to feed IST.

As stated above, the following aspects will be considered:

- the amount and type of the energy conversion devices to be installed: IST, having a bigger purchase power than a regular household, can achieve a cheaper price per device than single families;
- the buildings fit to be selected for the partnership: each building is characterized by several parameters defining the surface availability and its quality (a north-facing rooftop is less valuable than a non-shaded south-facing roof), as well as a number of apartments that have an energy

consumption profile;

- the share of investment cost to be split between IST and USRs;
- the economic conditions to which IST receives the EE from the USRs and vice-versa.

This work is structured as follows: Chapter 2 describes the system under investigation and the methods employed for its characterization, namely the procedures to process raw data and obtain the energy consumption profiles of the campus and the residential complexes and formulates the optimization problem. Chapter 3 describes how the simulation is performed, presents the results (including a sensitivity analysis) and reports the critical remarks. Finally in Chapter 4 conclusions are drawn.

Chapter 2

Methods

In this chapter the main procedures for the characterization of the system are presented. In 2.1 the system is described: the main hypotheses are shown, as well as the procedures to model IST and the USR's energy consumption profiles. Eventually in 2.3 the construction of the model is described in detail.

2.1 System description

The system is modeled as a central consumption node (the campus) surrounded by residential complexes that can become generation nodes and that, if so, will connect to it radially.

Fig. 2.1 shows the possible interactions between IST, a generic USR, and the grid. As shown, there can be an energy flow between IST and the selected USR. The arrows represent the possible directions of the energy flows (defined as P).

The IST campus has a peak EE consumption of 1 to 2 orders of magnitude greater than that of a single-family household: IST can be considered as a sink, therefore the extra EE that exceeds the requirements of a single household can always be accepted.

IST can be considered as a fictitious electricity storage system: with the exceeding EE produced by the over-sized PV modules, the USRs "charge" the campus which – when there is not solar energy production – can return the charged energy back to the respective USR. This is because IST generally pays a lower price per kWh than a common household. The IST-as-storage abstraction avoids a solution based on economic speculation: the price of energy the campus has access to – being a big consumer – is way lower than that of a private apartment, hence it could making profit just by selling at a higher price the energy it buys. This solution has not any added scientific value and would not have a positive impact on the grid system.

The system is modeled as a MILP problem: continuous variables are used for the energy and cash flows, and for the level of charge and volume of the thermal storage; integer variables are used for the number of PV modules and ST collectors that will be installed; binary variables are used for the selection of the USR and to model the variable unitary cost of energy along the day.

Superscripts and subscripts are to be read as "from-to", respectively.

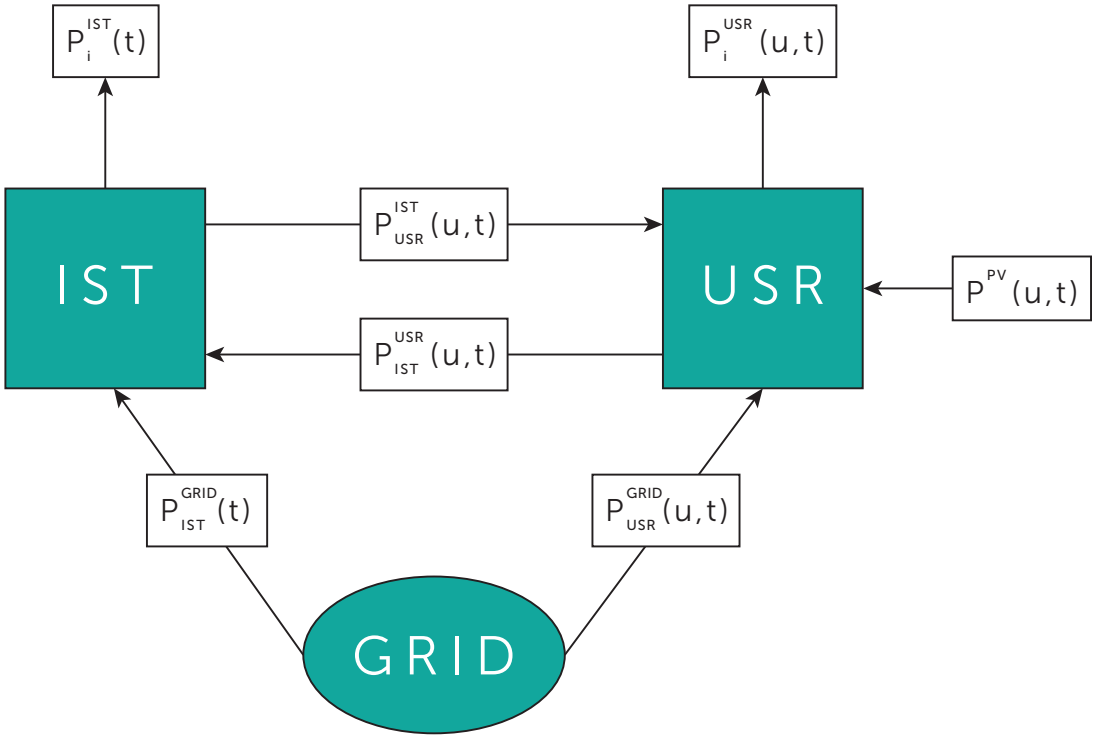

Figure 2.1: System representation.

2.1.1 Time horizon

The analysis is performed on a yearly basis, with 1 h resolution. With 8760 time steps to simulate a year, the computational effort (the solving time) would be too high. This is why it has been chosen to reduce the year to 4 representative "design" days, one for each season. This choice reduces greatly the complexity of the model. It has been shown that if the sequence of the design days along the year is not considered in the optimization problem – i.e. this is formulated independently for each design day – increasing their number does not lead to a change in the solution [31].

It has been chosen to limit the analysis to one year, as opposed to conducting it for the expected lifetime of the equipment (15 years) because of the unnecessary complications related to study such a long time period with an one-hour resolution and because one year is a sufficient amount of time to evaluate a system in all the possible states that can encounter throughout its lifetime. A similar behavior from year to year can therefore be expected.

The duration of the period under examination has been chosen to be of one year – instead of being the expected lifetime of the equipment (15 years) because one year is the minimum time

In the following subsections the process to the design day energy requirements will be explained.

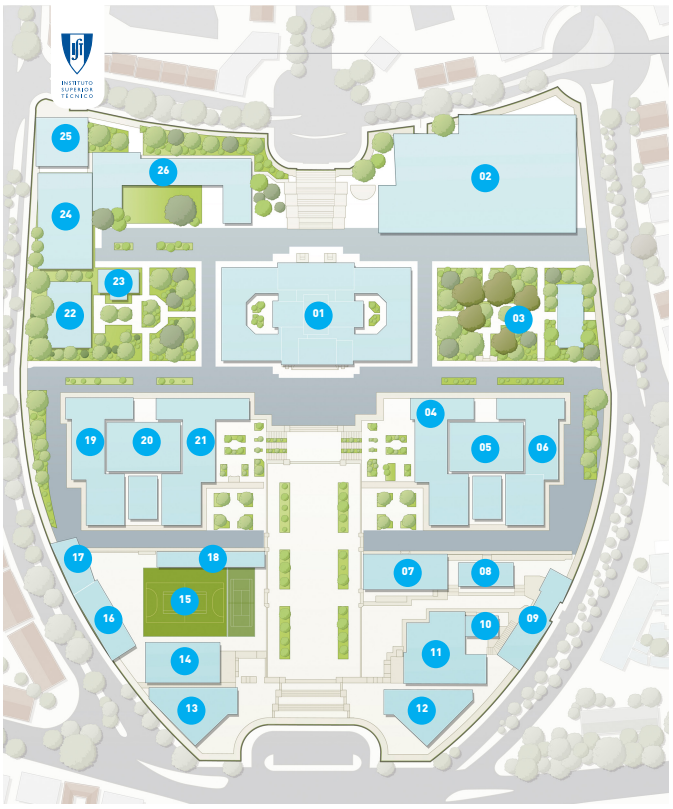

Figure 2.2: The Alameda campus of IST.

2.1.2 IST energy characterization

IST campus is situated on the top of a hill, and is composed of a total of 26 buildings (Pavilhões), in which didactic, research, or administrative activities take place. The plant of the campus can be seen in Fig. 2.2.

IST is characterized by an hourly electric energy demand. The "Campus Sustentável" project of IST [32] provided a file of hourly records of the campus electric demand. The measurements cover a time range from December 2015 to November 2017.

The raw data has been treated by removing the not-a-number (NaN) records. All the values that fall outside a $3\,\sigma$(99.7 % confidence) interval are removed because considered outliers, which are unusual values whose existence is to led back to random malfunctions of the measurement instruments and are not related to the phenomena of interest.

The records are grouped into seasons:

- winter ranges from 21/12 to 20/03;
- spring ranges from 21/03 to 20/06;
- summer ranges from 21/06 to 20/09[1];
- autumn ranges from 21/09 to 20/12;

This division of the year into seasons is consistent with the environmental records as explained later on in this section and shown in Fig. 2.9.

[1]The records of the month of August has been excluded: the two weeks closure and the absence of didactic activities make the month not representative of IST's normal functioning.

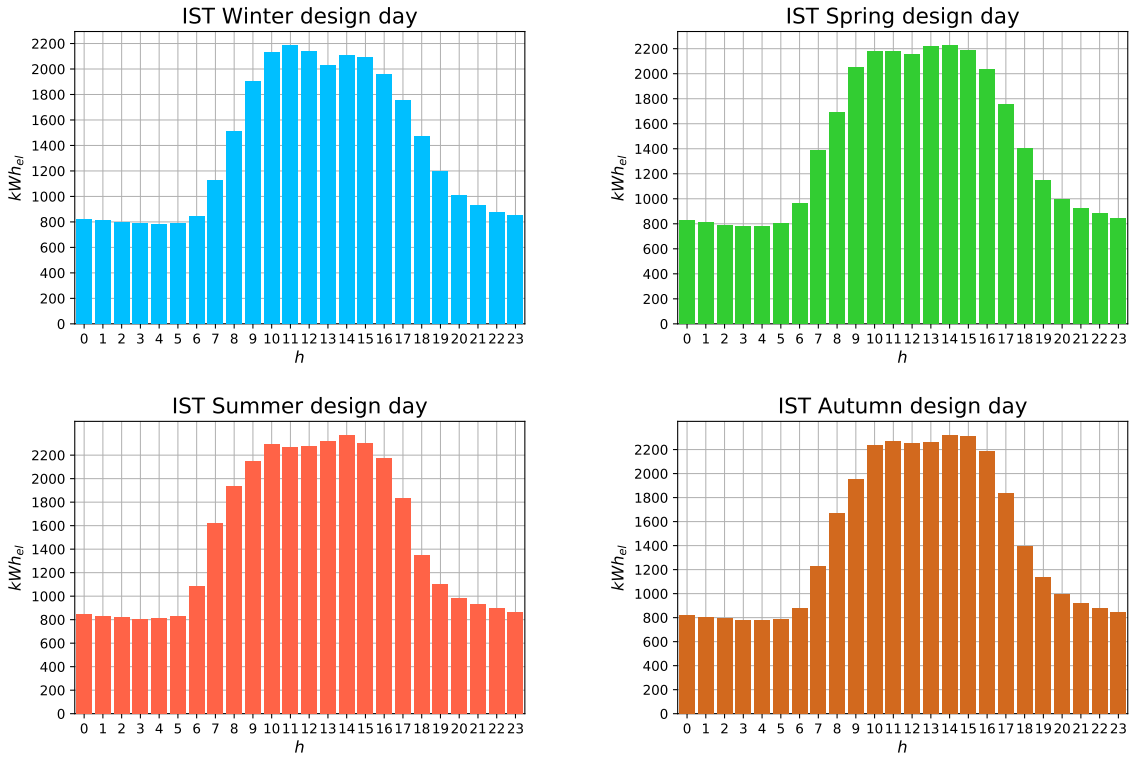

Figure 2.3: IST electrical consumption profiles for each season.

For each season, the records are again grouped by the hour of the day in which they were taken. For each of the 24 sets of each season, the median value is extracted: this value will be the value of the respective hour of the design day. The median has been preferred to the mean value due to its higher robustness and lower sensitivity on the extremes.

This process is represented in Fig. 2.4.

The resulting design days of this process are shown in Fig. 2.3. The obtained curves show that the daily EE consumption of the campus is rather constant along the year. This is consistent with the behavior of the campus, since it works for 11 months per year (in August the main activities are suspended). The base load is 800 kW, while the peak load is approximately 2.2 kW.

2.1.3 USR characterization

The city of Lisbon is made of thousands of buildings [33]: to characterize each one of them (single and multi-family residential, non-residential, ...) would require an in-depth analysis that is outside the scope of this work. It has been chosen to limit the number of USRs to four.

The four buildings have been picked following these criteria:

- vicinity to IST: lower distances mean lower losses, therefore the search for rooftops shall be focused on the surroundings of the campus;
- incident solar radiation: surfaces that receive large amounts of solar radiation over the year are more attractive than the others;

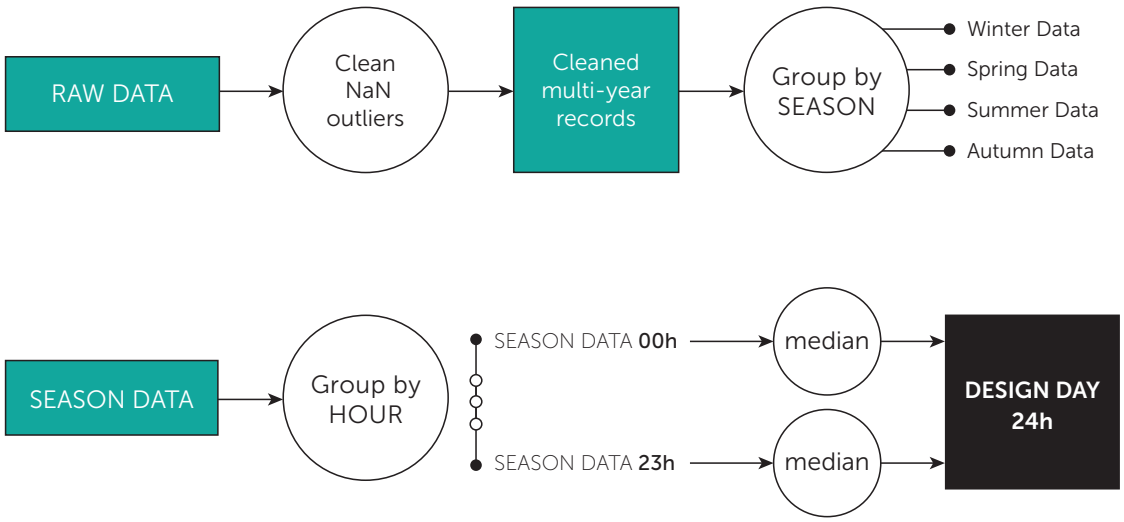

Figure 2.4: Representation of the procedure used to obtain the seasonal design days.

- representativity: the four buildings should not be unique, as the results from assessing a palace belonging to a family of constructions can be expected to be similar for the whole family.

This being said, the buildings that have been chosen are:

- USR_1: R. Visconde de Santarém, 24;
- USR_2: R. de Ponta Delgada, 51;
- USR_3: R. dos Açores, 46;
- USR_4: Av. Rovisco Pais, 16.

All of the constructions are situated to the south-facing side of the hill. They were all built between 1919 and 1945, and are referred as "gaioleiro" buildings [35], thus similar energetic performances can be expected. From observation, the number of floors and apartments has been derived.

Information regarding the amount of incident solar radiation on their respective roof as well as its surface extension was gathered from the "Solar Energy Potential" map [34]. The "Solar Energy Potential" map is a useful resource to gather data regarding the characteristics of the roofs of the city of Lisbon. A view of IST campus from the Solar Energy Potential map is presented in Fig. 2.5. Four classes are defined to discretize the rooftop surface of each building according to the amount of yearly incident solar radiation (I_y). These classes are:

- Class I (blue): $I_y \leq 1000\,\text{kWh}\,\text{m}^{-2}\,\text{year}^{-1}$;
- Class II (yellow): $1000\,\text{kWh}\,\text{m}^{-2}\,\text{year}^{-1} < I_y \leq 1400\,\text{kW}\,\text{m}^{-2}\,\text{year}^{-1}$;
- Class III (orange): $1400\,\text{kWh}\,\text{m}^{-2}\,\text{year}^{-1} < I_y \leq 1600\,\text{kW}\,\text{m}^{-2}\,\text{year}^{-1}$;
- Class IV (red): $I_y > 1600\,\text{kWh}\,\text{m}^{-2}\,\text{year}^{-1}$;

Figure 2.5: IST campus as seen from the solar energy potential map [34].

USR	ID	Floors	Flats	Tot. surface (m^2)	S_{III} (m^2)	S_{IV} (m^2)	γ (deg)
1	133	4	4	137.75	4.5	66.25	-5
2	25409	3	3	100.25	24.25	52	-60
3	52254	4	3	91.25	23	36.75	60
4	54937	5	8	264	23.75	119.5	0

Table 2.1: Characteristics of the buildings associated to the USRs.

The map is interactive (Fig. 2.6): the data of each building can be accessed by clicking on it. The informations that are displayed are:

- building identification number (ID_b);
- area of the roof (m^2);
- maximum value of I_y;
- minimum value of I_y;
- the amount of surface belonging to each class [[m^2].

The informations gathered for the USRs are shown in Tab. 2.1.

Electric load

Likewise for IST, the hourly electric energy demand for each USR was obtained from different sets of measurements. This data was provided by the *Center for Innovation, Technology and Policy Research* (IN+) of IST, that performed a range of measurements through the project “A sua casa, a sua energia”, promoted by ERSE [36]. The project monitored the energy consumption of the nation-wide participants with the purpose to improve the efficiency in the residential sector.

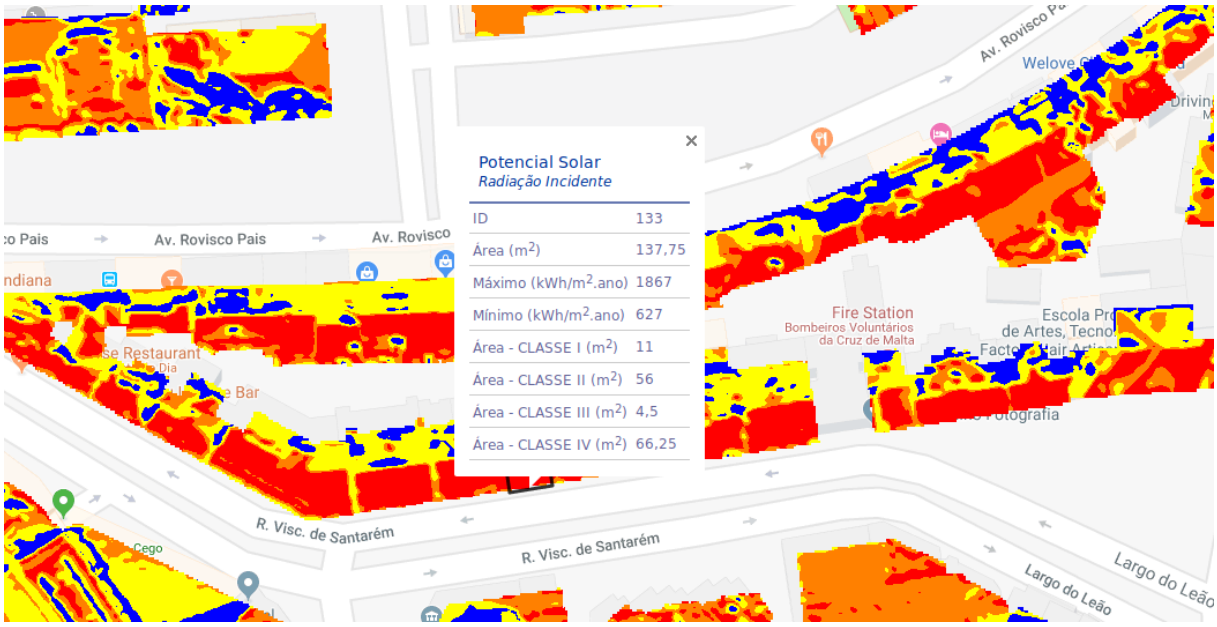

Figure 2.6: Detail of one of the constructions under study.

ID_{el}	Flat type	N of residents	Records time range
1057	T3	2	09/2012 – 09/2013
1062	T4+	3	01/2013 – 08/2014
1360	T2	3	10/2012 – 08/2015

Table 2.2: Electrical records selected for the USR's characterization.

From a pool of dozens of household consumption records, three criteria have been applied to discard the unfit households: the location (only the households situated in Lisbon were considered), the period covered by the measurements (due to the discontinuities of the records, only those households for each every month was recorded at least once), and the diversity (in case two or more flats were found to be fit according to the previous criteria, and they were of the same kind[2], the one with a greater amount of records was kept).

As a result of the selection process, the records fit for the analysis are shown in Tab. 2.2. The same process shown in 2.1.2 to obtain seasonal design days has been adopted. Fig. 2.7 shows the winter consumption curves obtained for each household considered. The results show that the energy consumption is proportional to the number of people living in the flat.

The measurements were performed on a set of electrical appliances. The files state that the monitored appliances were: 'washer', 'dishwasher', 'standby', 'fridge', 'rest'. This explains the relatively low peak energy consumptions, especially in winter, during the heating season. In fact, on a national scale, the use of EE for space heating is far greater than the natural gas [37]. Therefore, the electric consumption will be integrated with the energy consumption for space heating and domestic hot water (DHW)[3].

Eventually an electric profile has been associated to each USR. The association is based on the

[2]The flat type classification in Portugal is TN, where N means the number of rooms. Therefore a T4 is a flat with four bedrooms, a kitchen, a living room and a variable number of bathrooms. Similarly a T2 has only two bedrooms, a bathroom, a kitchen and so on.

[3]Even though the use of natural gas for DHW far exceeds the use of EE[37], it is assumed that each household only uses EE, for this means a higher electricity demand from the USRs, hence less favorable conditions.

USR	ID_b/ID_{el}	Type	Ppl/flat	N_{apt}	k
1	133/1057	T3	4	4	$2 \cdot 4$
2	25409/1057	T3	3	3	$3/2 \cdot 3$
3	52254/1360	T2	3	3	$1 \cdot 3$
4	54937/1062	T4+	4	8	$4/3 \cdot 8$

Table 2.3: Constant of proportionality for the electric consumption profile for each USR. ID_b is the ID of the building from [34], ID_{el} is the ID of the electric consumption profile provided by IN+, Ppl/flat is the number of people living in the respective flat, N_{apt} is number of apartments per building, k is the proportionality constant calculated with (2.1).

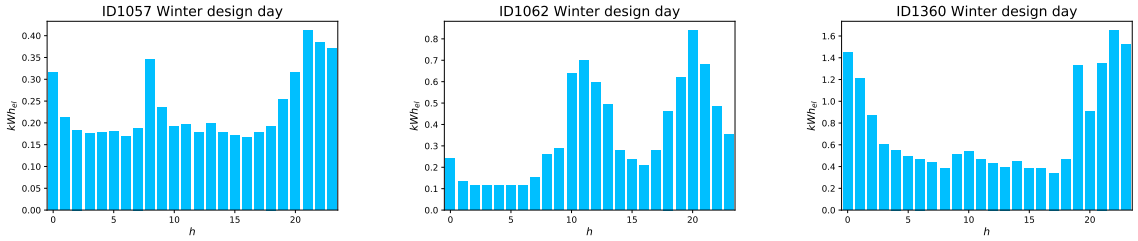

Figure 2.7: Winter design day electrical consumption for three different households.

following assumptions:

- the electric profile is proportional to the number of inhabitants: a profile can be adapted to a greater or lower number of residents through a proportionality constant;
- in a building all the flats are equal in terms of geometry (type), occupancy (number of people), and routines. Being $El._{1\ flat}$ the electric consumption profile for a single flat, the overall building consumption is:

$$P_{\text{USR}} = N_{\text{flats}} \cdot El._{1\ flat}.$$

- the design day electric consumption of a building can be therefore obtained by multiplying the respective profile by the proportional constant k:

$$k = \frac{N_{\text{residents}}}{N_{\text{residents profile}}} \cdot N_{\text{flats per building}}. \tag{2.1}$$

The results are shown in Tab. 2.3.

Thermal load

The daily thermal profile has been estimated with base on the weather data provided by IST Meteorological Service, the Portuguese regulations [6], and assumed U-values.

U-values Each building under examination belongs to the district of São Jorge de Arroios in Lisbon. The U-values were taken from [33], in which for each district of Lisbon a statistical analysis was performed. In this work, the minimum, mean, maximum, and std deviation values of the U-values for each district of

Lisbon are provided. Since the difference between the mean and the maximum U-values is minimal, the latter have been chosen, for the analysis to be more conservative.

The U-values therefore are:

- $U_{\text{wall}} = 2\,\text{W}\,\text{m}^{-2}\,\text{K}^{-1}$;
- $U_{\text{ceiling}} = 3\,\text{W}\,\text{m}^{-2}\,\text{K}^{-1}$;
- $U_{\text{floor}} = 3.3\,\text{W}\,\text{m}^{-2}\,\text{K}^{-1}$;
- $U_{\text{windows}} = 4.05\,\text{W}\,\text{m}^{-2}\,\text{K}^{-1}$;

All of the previous U-values exceed the maximum values indicated by the REH. This is because the REH only applies to "heavily renovated" or newly built buildings. It is not uncommon for constructions in "São Jorge de Arroios" to not have been "heavily" refurbished or renovated at all.

Additional assumptions were made: since all of the buildings taken into account are surrounded by two more buildings, the side walls were considered to be adiabatic; the glazing area equal to $GAP = 35\,\%$ of the total wall area, the infiltration and ventilation rate as $IR = 1.25\,\text{ACH}$ (air changes per hour), the height per floor as $h_f = 2.7\,\text{m}$, and the available floor area as the $90\,\%$ of the roof surface[4]: $AFA = 0.9 \cdot S_{\text{roof}}$.

The heating loss coefficient is then calculated as:

$$\begin{aligned} L = {} & (U_{\text{ceiling}} + U_{\text{floor}}) \cdot AFA + (1 - GAP) \cdot (UA)_{\text{wall}} + GAP \cdot (UA)_{\text{windows}} \\ & + AFA \cdot N_{\text{floors}} \cdot h_f \cdot \widehat{\rho}_{\text{air}} c_{p_{\text{air}}} \cdot \frac{IR}{3600} (\text{W}\,\text{K}^{-1}). \end{aligned} \tag{2.2}$$

Space heating load The thermal load is considered to be the result of two heating necessities: space heating (SH) and domestic hot water (DHW).

The approach used to determine the SH energy necessity is the one presented by Durmayaz et al., and it is described in Fig. 2.8.

From 5-years of hourly weather records for the city of Lisbon, a design-year has been extrapolated with the same procedure shown in 2.1.2.

Later, the daily mean temperatures where calculated for every day of the year. The values have been plotted and can be seen in 2.9. The daily temperature averages have been fitted with a $6\,\text{th}$-degree polynomial function. The beginning/end of the heating season has been identified for the days of the year in which the average temperature is below $15\,^{\circ}\text{C}$. The results is that the heating season ends on the $110\,\text{th}$ and begins on the $313\,\text{th}$ day, which corresponds to the $20\,\text{th}$ of April and $9\,\text{th}$ of November respectively. The resulting heating season is approximately $1\,\text{month}$ longer than what specified by the regulation.

The energy load for space heating is assumed to be proportional to the sum of degree-hours for the heating season [38]. The amount of degree-hours for the heating season is:

$$DH_{\text{season}} = \sum_{i=1}^{N} (T_{\text{ind}} - \overline{T}_i) \quad \text{for } \overline{T}_i \leq T_{\text{ref}}, \tag{2.3}$$

[4] It is reasonable to assume that $10\,\%$ of the surface inside the building is made of common areas (stairs, corridors) that are not heated.

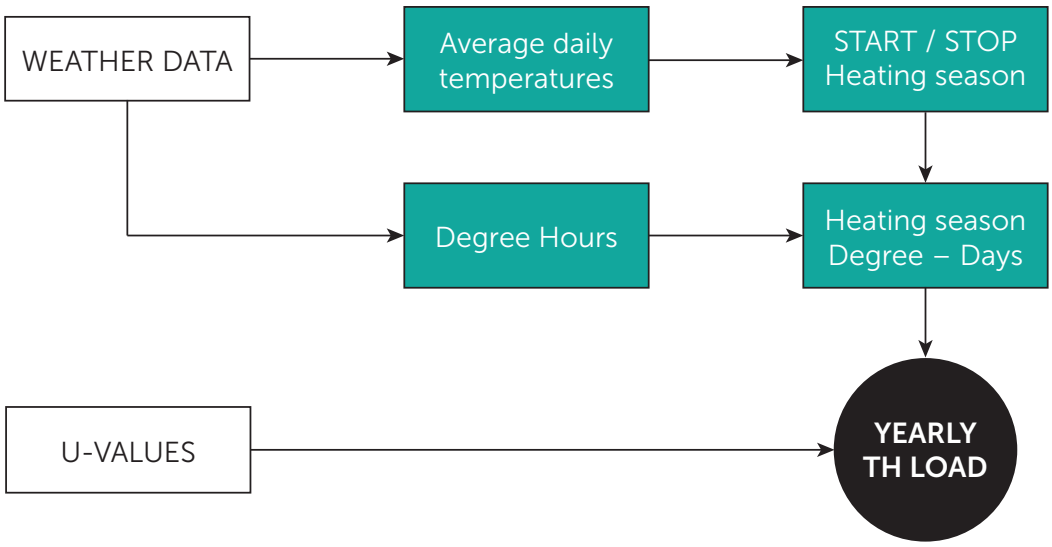

Figure 2.8: Algorithm for the calculation of the yearly space heating thermal load for a building.

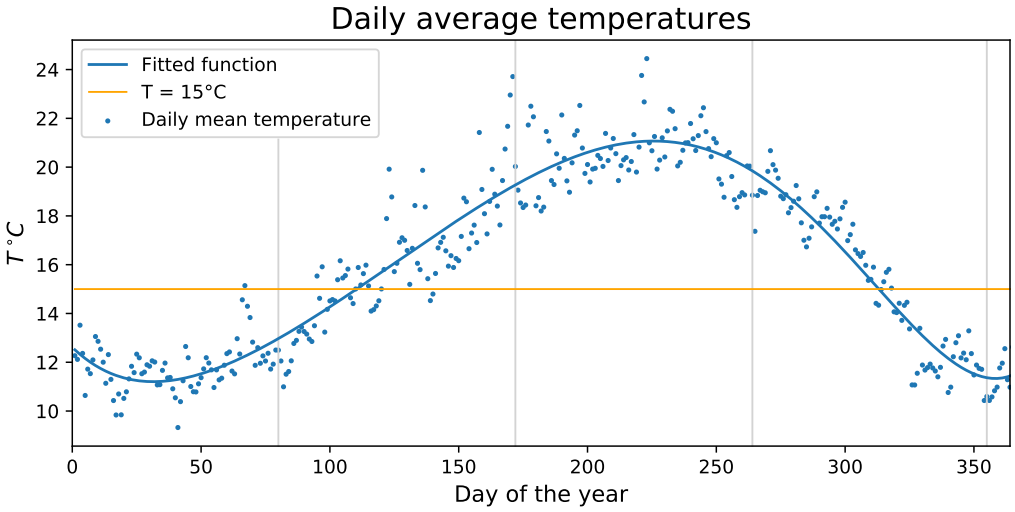

Figure 2.9: Yearly trend of the daily average temperatures. The vertical lines mark the ending of a season and the beginning of the next. Winter and summer cover the highest and lowest ranges of temperature levels respectively while spring and autumn cover the two transition periods.

USR	AFA (m^2)	A_{wall} (m^2)	L (kW m^{-2})	Q_{sh} (kWh)
1	123.98	91.8	1.589	79.077
2	90.23	64.8	1.051	69.727
3	82.23	59.4	1.049	69.581
4	237.60	202.50	3.3838	67.350

Table 2.4: Space heating thermal load for each USR.

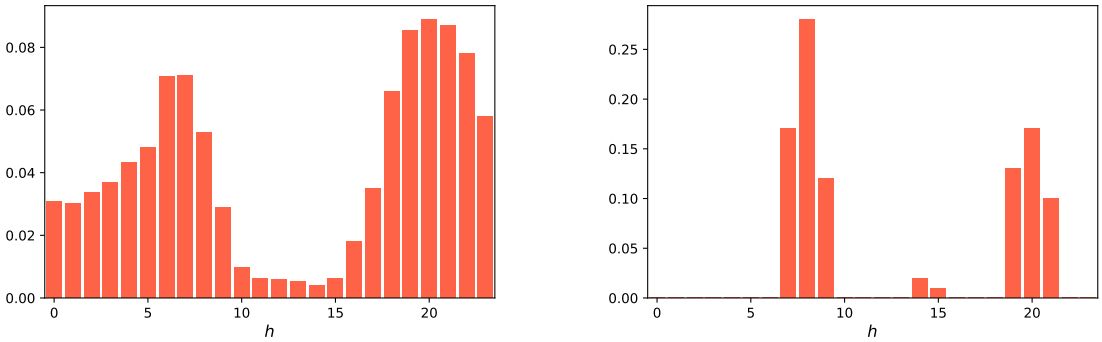

(a) Space heating.

(b) Domestic hot water.

Figure 2.10: Normalized hourly thermal energy consumption profiles.

where T_{ind} is the constantly adopted indoor design air temperature (20 °C according to the REH), $\overline{T}_i$ is the i-th hourly mean temperature of the heating season, and T_{ref} is the base temperature for the beginning/end of the heating season, 15 °C.

The average temperature of every design day is above 15 °C except for the winter one. The winter season is the only entirely inside the heating season, therefore the space heating load will only be present for the winter design day. The number of DH of the heating season corresponds to the sum of the DH of every day in it, this ensures the following property:

$$\frac{Q_{\text{dd}}}{Q_{\text{season}}} = \frac{DH_{\text{dd}}}{DH_{\text{season}}}, \tag{2.4}$$

which means that the energy required for space heating for the winter design day is:

$$Q_{sh} = L \cdot DH_{\text{dd}}. \tag{2.5}$$

It is worth making a further correction: it is unusual for a Portuguese household to heat the entire flat. It has been chosen to apply a correction factor of $1/3$ to the Q_{sh} to take into account the non-heated parts of the respective flats.

Eventually, the normalized space heating profile shown in Fig. 2.10a has been applied to obtain the daily space heating energy consumption.

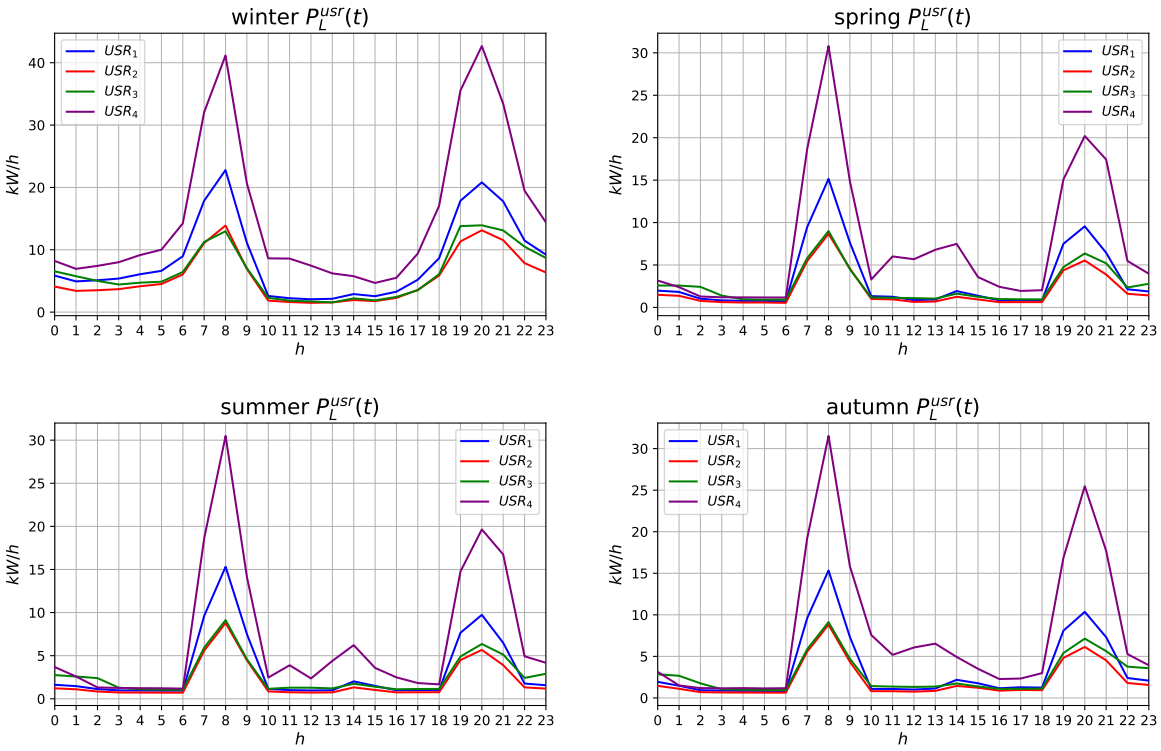

Figure 2.11: Overall electric load of of each USR for each season (assuming all the heat demand is fulfilled with electric energy.

Domestic hot water load For the DHW energy consumption, the daily amount of energy has been calculated according to the REH:

$$Q_{dhw}(\text{kWh d}^{-1}) = 60\,\text{L/pers} \cdot N_{\text{people}} \cdot c_{p,\text{water}} \cdot (60\,^{\circ}\text{C} - 15\,^{\circ}\text{C}) \cdot \frac{1}{3600}\text{h s}^{-1}, \tag{2.6}$$

The the municipal water feed temperature and the normalized profile for the DHW consumption (Fig. 2.10b) were retrieved from [39].

If all the thermal load were to be fulfilled with EE (through an electrical resistance of $98\,\%$ efficiency), the overall electrical consumption profile for each USR in each design day would be the one presented in Fig. 2.11.

2.2 Renewable energy production

The specific solar energy production per unit equipment is modeled as a function of the solar radiation and ambient temperature. Both data sets have been recorded over a period of 5 years by the Meteorological Service of IST. The detailed model of the off-design energy conversion of both PV and ST modules is presented in Appendix A.

2.3 Formulation of the optimization problem

A MILP description of an optimization problem starts with fixing all the parameters – constant and known a priori – and then choosing the decision variables – whose optimum value will be found. A MILP optimization problem can be written in a general form as:

find $\mathbf{x(t)}$ *which minimizes:*

$$\begin{aligned} Z &= f(\mathbf{x(t)}) \\ s.t. \quad g(\mathbf{x(t)}) &= 0 \\ h(\mathbf{x(t)}) &\leq 0, \end{aligned} \tag{2.7}$$

where Z is the objective function, $\mathbf{x(t)}$ the array of the decision variables' optimum value, while $g(\mathbf{x(t)})$ and $h(\mathbf{x(t)})$ are respectively the equality and inequality constraints deriving from the model of the system.

2.3.1 Objective function

The objective function, to minimize, is the annual costs for energy of IST:

$$Z = C_{inv+O\&M} + C_{el,grid} - Rev^{ist}_{usr}, \tag{2.8}$$

where $C_{inv+O\&M}(u)$ is the overall investment and operation and maintenance cost (expressed as a percentage of the former) for each USR, $C_{el,grid}$ are the costs from the purchase of EE from the grid and Rev^{ist}_{usr} are the revenues from the sale of EE to the USRs.

The costs in (2.8) are:

$$C_{inv+O\&M} = \sum_{u} (C^{inv}_{pv}(u) + C^{inv}_{st}(u)) \cdot (1 + 0.05) \tag{2.9}$$

$$C_{el,grid} = \sum_{t} P^{grid}_{usr}(u,t) \cdot \widehat{c}^{ist}_{el}(t) \tag{2.10}$$

$$Rev^{ist}_{usr} = \sum_{u} \sum_{t} P^{ist}_{usr}(u,t) \cdot \widehat{c}^{usr}_{el}(t). \tag{2.11}$$

The term $(1 + 0.05)$ in (2.9) represents the overall cost of the investment and the O&M costs, which for the solar technology, has been imposed $5\,\%$ [31].

The investment costs are:

$$C^{inv}_{pv}(u) = \sigma(u) \cdot \widehat{c}_{pv} \cdot \widehat{W}_p \cdot \widehat{r}_t \tag{2.12}$$

$$C^{inv}_{st}(u) = (\chi(u) \cdot \widehat{c}_{st} + V_{ts,max}(u) \cdot \widehat{c}_{ts}) \cdot \widehat{r}_t, \tag{2.13}$$

with

$$\widehat{r}_t = \frac{i \cdot (1+i)^n}{(1+i)^n - 1)}. \tag{2.14}$$

$\widehat{W}_p$ is the peak wattage of the selected PV technology, which in this case is equal to $290\,\mathrm{Wp}$ [40]. $\widehat{r}_t$ is the actualization factor. $V_{ts,max}(u)$ is the maximum capacity of the TS and corresponds to the optimal volume

of the storage oversized by $10\,\%$ (for prudence):

$$V_{ts,max}(u) = V_{ts}(u,t) \cdot 1.1. \tag{2.15}$$

2.3.2 Fixed parameters

The parameters are those quantities that are known beforehand, they are:

- Electric consumption (load) for IST and each USR ($\widehat{P}_L^{ist}(t),\ \widehat{P}_{el}^{usr}(u,t)$ [kWh$_{el}$]);
- SH and DHW thermal loads for each USR ($\widehat{Q}_L^{sh}(u,t),\ \widehat{Q}_L^{dhw}(u,t)$ [kWh$_{th}$]);
- Initial charge level: $LVL(u,-1)$[kWh]
- Energy production per module/collector of PV and ST technologies ($\widehat{p}_{pv}(u,t)$, $\widehat{q}_{st}(u,t)$ [kWh N^{-1}]) and their unitary surface ($\widehat{A}_{mod}, \widehat{A}_{coll}$ [m^2/(unit)]);
- Hot and cold temperatures in the TS ($\widehat{T}_h, \widehat{T}_c$ [°C]);
- Available roof surface for each USR ($\widehat{S}(u)$ [m^2]);
- Round-trip efficiency for the charge and discharge of the heat storage equipment ($\widehat{\eta}_{ts} = \widehat{\eta}_{ch} \cdot \widehat{\eta}_{disch}$);
- Physical properties of water ($\widehat{\rho}_w$ [kg m^{-3}], $\widehat{c}_{p,w}$ [kJ kg^{-1} K^{-1}]);
- Efficiency of EE transmission ($\widehat{\eta}_{el,t}$);
- Efficiency of the electrical resistance heater ($\widehat{\eta}_{el,c}$);
- Unitary costs of PV modules and ST collectors ($\widehat{c}_{pv}$[€ Wp^{-1}], $\widehat{c}_{st}$ [€ N^{-1}]);
- Specific cost of TS ($\widehat{c}_{ts}$ [€ m^{-3}]);
- Prices for the EE withdrawn from the grid, for both IST and USRs ($\widehat{c}_{el}^{ist}(t)$ $\widehat{c}_{el}^{usr}(t)$ [€/kWh$_{el}$]);
- Interest rate and expected lifetime of the equipment ($i,\ n$ [year]);
- A very big number $\widehat{M}$.

The parameters which are constant with the time are presented in Tab. 2.5. $\widehat{c}_{pv}$ is the specific cost per watt-peak of a PV module, and it includes the cost for the module itself, the auxiliaries, and the installation costs. Its value has been chosen as the most expensive price found in [41]. The price of the EE varies with the hour of the day. IST has a 4-phase tariff contract with the energy provider: *ponta, cheia, vazio, super vazio*. The USRs are assumed to have a 2-phase contracts: *vazio, fora de vazio*:

- winter time 4-phase tariff:
  - *ponta*: 09:00 to 10:30, 18:00 to 20:30;
  - *cheia*: 08:00 to 09:00, 10:30 to 18:00, 20:30 to 22:00;
  - *vazio*: 00:00 to 02:00, 06:00 to 08:00, 22:00 to 00:00;

	Unit	Value
$LVL(u,-1)$	[kWh]	100
$\widehat{T}_h$	[°C]	15
$\widehat{T}_c$	[°C]	60
$\widehat{\rho}_w$	[kg m^{-3}]	1000
$\widehat{c}_{p,w}$	[kJ kg^{-1} K^{-1}]	4.186
$\widehat{\eta}_{ts}$	—	0.95
$\widehat{\eta}_{el,t}$	—	0.98
$\widehat{\eta}_{el,c}$	—	0.98
$\widehat{c}_{pv}$	[€ Wp^{-1}]	2
$\widehat{c}_{st}$	[€/coll]	400
$\widehat{c}_{ts}$	[€ m^{-3}]	2000
i	[%]	7
n	[years]	15

Table 2.5: Parameters constant with the time.

$\widehat{c}_{el}^{ist}$	[€/kWh$_{el}$]	$\widehat{c}_{el}^{usr}$	[€/kWh$_{el}$]
ponta	0.327	f. de vazio	0.1948
cheia	0.099	vazio	0.1009
vazio	0.07		
s. vazio	0.061		

Table 2.6: Time-dependent prices of energy.

  - *super vazio*: 02:00 to 06:00;

- summer time 4-phase tariff:

  - *ponta*: 10:30 to 13:00, 19:30 to 21:00;
  - *cheia*: 08:00 to 10:30, 13:00 to 19:30, 21:00 to 22:00;
  - *vazio*: 00:00 to 02:00, 06:00 to 08:00, 22:00 to 00:00;
  - *super vazio*: 02:00 to 06:00.

As for the spring and autumn seasons, summer and winter time tariffs have been applied.

All the USRs have a 2-phase tariff: *vazio, fora de vazio*. All along the year the *vazio* period lasts from 22:00 to 08:00.

The cost for each phase are shown in Tab. 2.6. For IST's *ponta* phase the price is composed of two parts: the energy component (0.112 € kWh^{-1}) and the power component (0.215 € kW^{-1}). Since the model is based on an houly time-step it is possible to sum the two components and obtain an overall price per kWh.

2.3.3 Decision variables

The complete decision variables set of optimization problem includes the following different variable types: continuous, integer and binary.

The continuous variables describe the energy flows, the amount of stored energy in IST and in the TS devices, and for sizing the latter. Integer variables are used for the number of equipment to be installed: PV modules and ST collectors, and binary variables for the inclusion/exclusion of candidate USRs in the system.

Continuous variables

- Energy flow from grid to IST : $P_{ist}^{grid}(t)$;
- Energy flow from USR to IST: $P_{ist}^{usr}(u,t)$;
- Energy flow from IST to USR: $P_{usr}^{ist}(u,t)$;
- Energy flow from grid to USR: $P_{usr}^{grid}(U,t)$;
- Thermal energy generated by USR's electric heater: $Q^{eh}(u,t)$;
- Thermal energy dissipated to the environment: $Q^{diss}(u,t)$;
- Thermal energy charged into the TS: $Q_{ch}^{ts}(u,t)$;
- Thermal energy discharged from the TS: $Q_{disch}^{ts}(u,t)$;
- Level of charge of the TS: $LVL_{ts}(u,t)$;
- Volume of the TS: $V_{ts}(u,t)$;
- Amount of energy credit that a USR has towards IST (level of charge): $LVL(u,t)$;

Integer variables

- Number of the installed PV modules: $\sigma(u)$;
- Number of the installed ST modules: $\chi(u)$.

Binary variables

- Decision variable for the association between IST and USR to exist: $\alpha(u)$;
- Decision variable for developing a ST system: $\varepsilon(u)$;
- Accessory variables to exclude contemporaneity of opposite energy flows: $s_{el}(u,t)$, $s_{th}(u,t)$.

2.3.4 Constraints

Constraints are linear functions setting conditions that variables are required to satisfy. In this problem, the constraints are used to impose the conditions under which the system can exist and operate, such as the energy balances and flows, the usage of the available roof surface, and the economic conditions.

Energy balances

There are three energy balances: two electrical (for IST and for each USR) and one thermal (only for USR). In fact, the possibility to develop a district heating network is not contemplated in this work.

IST el. en. balance:

$$\widehat{P}_L^{ist}(t) + \sum_u P_{usr}^{ist}(u,t) - \widehat{\eta}_{el,t} \cdot \sum P_{ist}^{usr}(u,t) - P_{ist}^{grid}(t) = 0. \tag{2.16}$$

USR el. en. balance:

$$P_L^{usr}(u,t) + P_{ist}^{usr}(u,t) - \widehat{\eta}_{el,t} \cdot P_{usr}^{ist}(u,t) - P_{pv}(u,t) - P_{usr}^{grid}(u,t) = 0, \tag{2.17}$$

where:

$$P_L^{usr}(u,t) = \widehat{P}_{el}^{usr}(u,t) \cdot \alpha(u) + \frac{Q_{eh}(u,t)}{\widehat{\eta}_{el,c}} \tag{2.18}$$

$$P_{pv}(u,t) = \widehat{p}_{pv}(u,t) \cdot \sigma(u). \tag{2.19}$$

USR th. en balance:

$$Q_L^{usr}(u,t) \cdot \alpha(u) - Q^{st}(u,t) - Q^{eh}(u,t) - Q_{disch}^{ts}(u,t) + Q_{ch}^{ts}(u,t) + Q^{diss}(u,t) = 0 \tag{2.20}$$

where:

$$Q_L^{usr}(u,t) = \widehat{Q}_L^{sh}(u,t) + \widehat{Q}_L^{dhw}(u,t) \tag{2.21}$$

$$Q^{st}(u,t) = \widehat{q}_{st}(u,t) \cdot \chi(u) \cdot \widehat{A}_{coll}. \tag{2.22}$$

The binary variable $\alpha(u)$ appears in (2.18) and (2.20) serves to set the USR's demand equal to zero when it is not selected to form the cooperative ($\alpha(u) = 0$).

Energy flows management

$$P_{ist}^{usr}(u,t) \leq P_{pv}(u,t) \tag{2.23}$$

$$P_{usr}^{ist}(u,t) \leq \left(\widehat{P}_{el}^{usr}(u,t) + \frac{\widehat{Q}_L^{sh}(u,t) + \widehat{Q}_L^{dhw}(u,t)}{\widehat{\eta}_{el,c}} \right) \cdot \alpha(u) \tag{2.24}$$

$$Q^{eh}(u,t) \leq Q_L^{usr}(u,t) \cdot \alpha(u) \tag{2.25}$$

$$Q^{diss}(u,t) \leq Q^{st}(u,t). \tag{2.26}$$

Constraint (2.23) is necessary to exclude the possibility that the USR sends EE to IST by purchasing it from the grid, similarly (2.24) is necessary so that IST does not send energy to a USR that has not been selected (because in the simulation all the USR start with a certain energy credit form IST): when the

USR is not selected, there shall not be any interaction with IST. The energy consumption of the auxiliary heater when the USR is not selected is set to zero by (2.25), and the dissipated energy is null if there is not renewable solar thermal energy production by 2.26 .

Roof surface management

$$\sigma(u) \cdot \widehat{A}_{mod} + \chi(u) \cdot \widehat{A}_{coll} \leq \widehat{S}(u) \tag{2.27}$$

$$\sigma(u) \cdot \frac{\widehat{A}_{mod}}{\widehat{S}(u)} \leq \alpha(u) \tag{2.28}$$

$$\chi(u) \cdot \frac{\widehat{A}_{coll}}{\widehat{S}(u)} \leq \varepsilon(u) \tag{2.29}$$

$$\varepsilon(u) \leq \alpha(u) \tag{2.30}$$

Constraint (2.27) states that the overall surface covered by modules and collectors has to be lower or equal than the available amount. If a USR is not selected then the amount of modules is null thanks to (2.28), but if the roof is selected priority is given to the PV rather than to the ST thanks to (2.29) and (2.30).

IST as storage

Each USR begins the day with an initial energy credit of 100 kWh: this allows IST to send electrical energy to the USRs during the whole night, and not just until midnight.

$$LVL(u,t) = LVL(u,t-1) + \widehat{\eta}_{el,t} \cdot P^{usr}_{ist}(u,t) - P^{ist}_{usr}(u,t) \tag{2.31}$$

$$LVL(u,0) \leq LVL(u,23) \tag{2.32}$$

$$P^{ist}_{usr}(u,t) \leq \widehat{M} \cdot s_{el}(u,t) \tag{2.33}$$

$$P^{usr}_{ist}(u,t) \leq \widehat{M} \cdot (1 - s_{el}(u,t)) \tag{2.34}$$

Since IST is modeled as a sink, it is capable to accept all the energy that exceeds the consumption of the respective USR. If the campus should behave like a storage device, it would release up to the amount of energy it was charged with. When there is no production, IST can purchase energy from the grid and sell it to the respective USR, until all the stored energy during the day is returned. This behavior is modeled by (2.31). Equation (2.32) is a consequence of IST being a fictitious storage: the energy conservation does not apply, and the campus should not release more energy than received. The last two constraints – (2.33) and (2.34) – mandate that the energy can not be flowing in both senses at the same time.

Thermal storage

The model of the TS consists in two energy balances: between two subsequent hours and between the beginning and the end of the day:

$$LVL_{ts}(u,t) = LVL_{ts}(u,t-1) + \frac{3600\,\mathrm{s\,h^{-1}}}{\widehat{\rho}_w \cdot \widehat{c}_{p,w} \cdot (T_h - T_c)} \cdot \\ \cdot (\widehat{\eta}_{ts} \cdot Q^{ts}_{disch}(u,t) - \frac{1}{\widehat{\eta}_{ts}} \cdot Q^{ts}_{ch}(u,t)) \tag{2.35}$$

$$LVL_{ts}(u,0) = LVL_{ts}(u,23) \tag{2.36}$$

$$V_{ts}(u,t) = V_{ts}(u,t-1) + \frac{3600\,\mathrm{s\,h^{-1}}}{\widehat{\rho}_w \cdot \widehat{c}_{p,w} \cdot (T_h - T_c)} \cdot \\ \cdot \sum_t (\widehat{\eta}_{ts} \cdot Q^{ts}_{disch}(u,t) - \frac{1}{\widehat{\eta}_{ts}} \cdot Q^{ts}_{ch}(u,t)) \tag{2.37}$$

$$Q^{ts}_{disch}(u,t) \leq \widehat{M} \cdot s_{th}(u,t) \tag{2.38}$$

$$Q^{ts}_{ch}(u,t) \leq \widehat{M} \cdot (1 - s_{th}(u,t)). \tag{2.39}$$

The stored energy is represented as the amount of hot water in the tank: the second term of eq. (2.35) is the sum between the amount of stored energy on the previous hour and the variation of water in the tank. The charged and discharged thermal flows are multiplied for the round-trip efficiencies. Their difference is then multiplied by a constant: on the numerator there is the term to convert J to kWh, while on the denominator the thermo-physical properties of the water (density, specific heat, and temperature difference between the heated and feed water). Similarly, eq. 2.37 is used to design the volume of the storage, the main difference being that the final value of the volume will be the maximum of the obtained series of hourly volumes. Eventually, inequalities (2.38) and (2.39) are akin to (2.33) and (2.34).

Economical constraints

The following constraint imposes that – for the solution to be feasible – the USR has to save money compared to the case in which there is no intervention, and it purchases all of the energy from the grid:

$$\sum_t (P^{grid}_{usr}(u,t) \cdot \widehat{c}^{usr}_{el}(t)) \leq \sum_t (P^{usr}_{L}(u,t) \cdot \widehat{c}^{usr}_{el}(t)) \tag{2.40}$$

Bounds

$$P_{ist}^{grid} \geq 0 \tag{2.41}$$

$$P_{ist}^{usr}(u,t) \geq 0 \tag{2.42}$$

$$P_{usr}^{ist}(u,t) \geq 0 \tag{2.43}$$

$$P_{usr}^{grid}(U,t) \geq 0 \tag{2.44}$$

$$R_{usr}^{ist}(u,t) \geq 0 \tag{2.45}$$

$$Q^{eh}(u,t) \geq 0 \tag{2.46}$$

$$Q^{diss}(u,t) \geq 0 \tag{2.47}$$

$$Q_{ch}^{ts}(u,t) \geq 0 \tag{2.48}$$

$$Q_{disch}^{ts}(u,t) \geq 0 \tag{2.49}$$

$$LVL_{ts}(u,t) \geq 0 \tag{2.50}$$

$$V_{ts}(u,t) \geq 0 \tag{2.51}$$

$$\sigma(u) \geq 0 \tag{2.52}$$

$$\chi(u) \geq 0, \tag{2.53}$$

The optimization model was implemented in Python and solved using the MIP solver of GUROBI, which employs a branch and bound algorithm.

Chapter 3

Simulations and results

3.1 Simulations

The model is tested on four design days representative of one year: each design day is simulated independently, the resulting value of the objective function is multiplied by the number of days in the season and eventually the four results are summed. Following this approach, eq. (2.8) becomes:

$$Z = \sum_{s} \left(\sum_{u} C_{inv+O\&M} \cdot \frac{1}{365} + C_{el,grid} - Rev_{usr}^{ist} \right) N_{\text{days}}, \ \forall s \in \{seasons\}. \tag{3.1}$$

The simulations are performed in two steps:

1st step Each season is simulated independently. This results in a solution in which the decision variables change according to the season. This is the optimal solution. The number of installed equipment can not change along the year and therefore it is not viable;

2nd step Each season is simulated again, with the decision variables fixed as parameters with the values obtained by the previous simulation: this equals to design the system according to a season in particular.

Four solutions are obtained, where the optimum one corresponds to the minimum value of the objective function. The simulations were performed on a machine with a Intel Core i7-3517U $1.90\,\text{GHz}$ quad core processor. The solving time of each simulations is below $1\,\text{s}$.

3.2 Results

For every simulation performed, every USR is selected to form a cooperative with IST. The ST system, as well as the TS, are never part of the optimal solution: the focus is entirely on the electrical energy production.

	USR_1	USR_2	USR_3	USR_4
σ_{winter}	42	1	1	54
σ_{spring}	42	59	35	85
σ_{summer}	42	59	35	85
σ_{autumn}	29	8	1	85
Yearly savings (%)	28.30	8.71	23.46	27.48

Table 3.1: Results of the 1st step simulation: number of PV modules to be installed and yearly savings on the energy-related costs.

3.2.1 Base scenario

The reference situation for the calculation of the savings is the case of no-intervention: IST and the USRs are connected to the grid and they purchase all the energy they need. In this scenario:

- IST spends $1\,684\,246.44\,€\,\text{year}^{-1}$;
- USR_1 spends $6581.048\,€\,\text{year}^{-1}$;
- USR_2 spends $4181.554\,€\,\text{year}^{-1}$;
- USR_3 spends $4991.068\,€\,\text{year}^{-1}$;
- USR_4 spends $13\,942.419\,€\,\text{year}^{-1}$.

3.2.2 First step solution

The number of PV modules (that are $\sigma(u)$) part of the optimal solution are presented in Tab. 3.1. With this configuration it is found that IST saves the $0.312\,\%$ of yearly energy-related costs, while the USRs between the 8 and the $28\,\%$. USR_2 has a lower monetary saving because the building surface has an azimuth angle tilted 60 East: the peak power production is shifted before noon: this results in beginning the self-consumption of renewable energy before the beginning of the least favorable tariff phase (which starts at 08:00).

3.2.3 Second step solution

After running the simulation for the three cases (winter, spring-summer, winter), it is found that the optimal configuration is the spring-summer: all the available surface is covered with PV modules.

The total installed capacity is $64.09\,\text{kWp}$, for an initial investment of $128\,180\,€$. By implementing this solution, the yearly savings in the cost of energy will be:

- for IST: $0.276\,\%$
- for USR_1: $28.351\,\%$
- for USR_2: $24.472\,\%$
- for USR_3: $28.78\,\%$

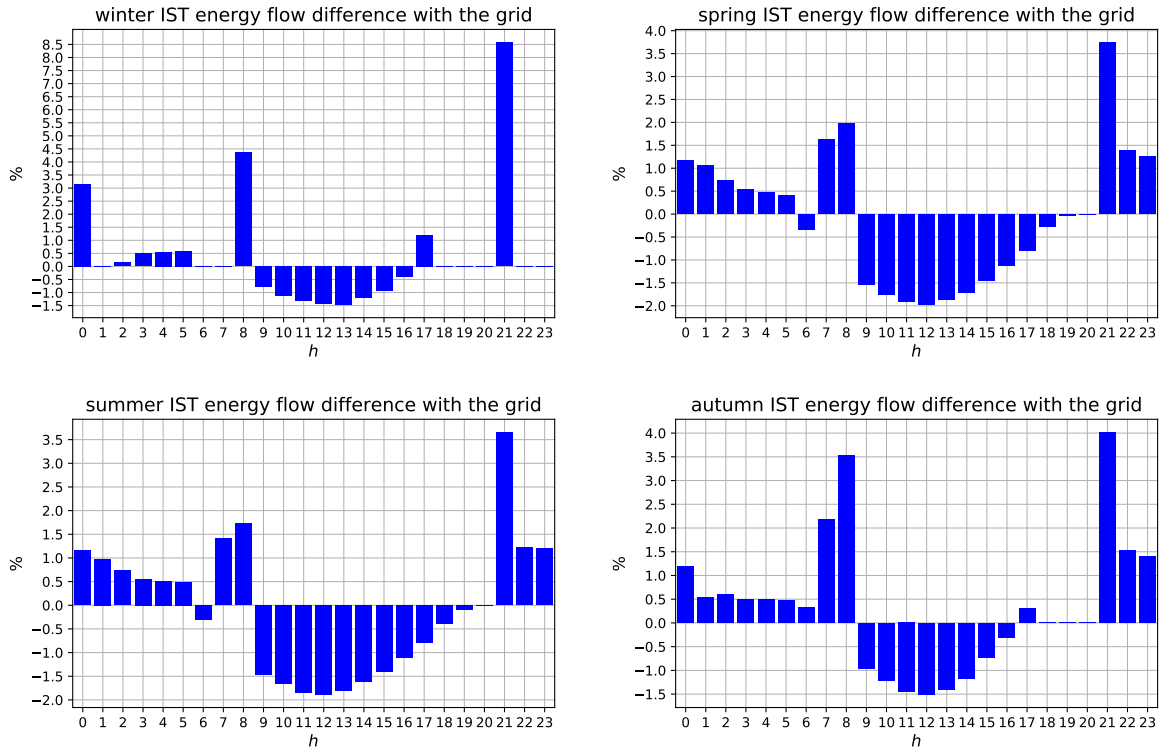

Figure 3.1: IST percentage variation of the energy purchased from the grid.

- for USR_4: 27.522 %

The energy purchased by IST from the grid decreases during the PV production time, while it increases in correspondence of the peak electricity demand from the USRs, as shown in Fig. 3.1. The *ponta* phase occurs from 18:00 to 20:30, it can be seen that in autumn and winter, when the sunset occurs before that time, the variation of energy purchased is null: IST waits for the most expensive phase to finish before feeding back the USRs with the energy it has accumulated.

Results show that USR_2 is the most suitable user for integration with IST: its electricity demand profile is not very different that of USR_3 (see Fig. 2.11), but the amount of stored energy profile is remarkably different, as in Fig. 3.2. This is due to the different and opposite azimuth angle of the surfaces: the USR_2's peak of PV energy production can cover the morning peak (completely in spring and summer, partially in autumn), on the other hand the USR_3's surface orientation does not provide benefits with respect to the evening peak (at 20:00) as shown in Fig. 3.3.

IST being a fictitious storage system has the advantage that it is not constrained by the law of conservation of energy: the campus can receive unlimited amounts of energy and release as much as it is convenient to. In this framework, on IST's perspective, the most attractive partners would be those that make the level of charge increase from the beginning to the end of the day. USR_2 is the most attractive of the set of USRs in this regards: it is the only one that gives a positive contribution to the daily energy stored by IST for three seasons out of four (whereas the others manage to do so only in spring and summer, the most favorable). These results suggest that, for such electricity consumption profiles and tariffs, USRs with East-oriented surfaces are preferable for IST.

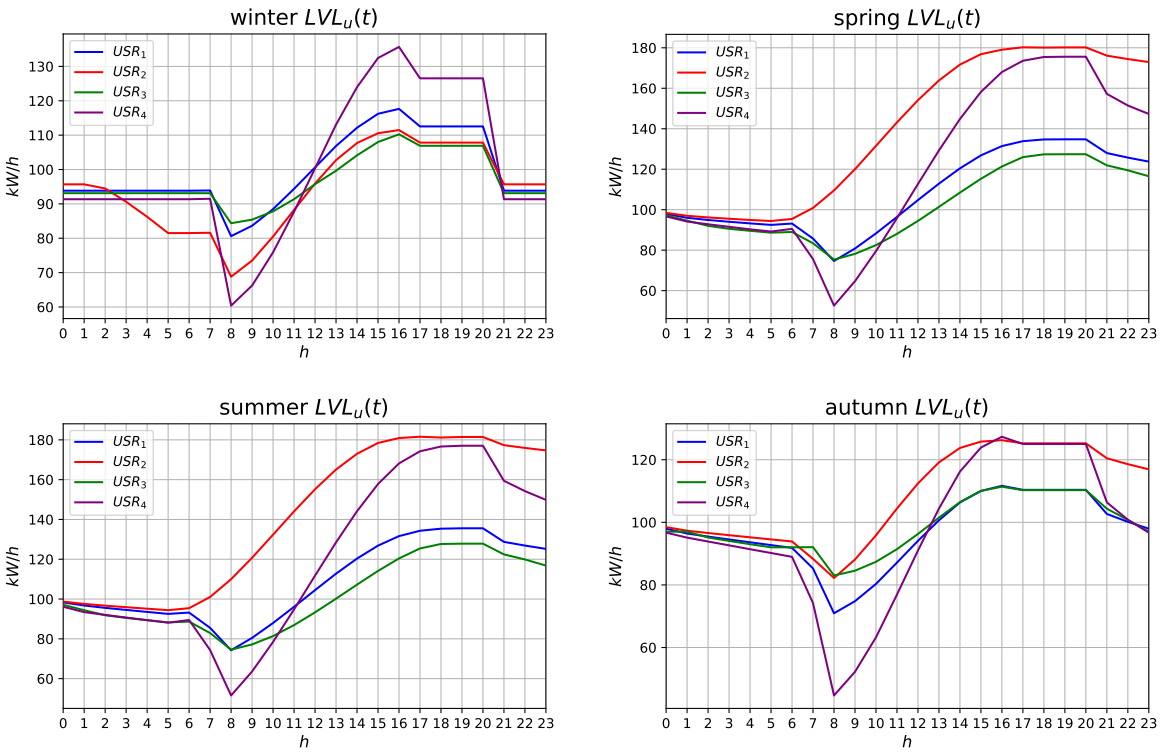

Figure 3.2: Level of charge of the IST as a fictitious storage system.

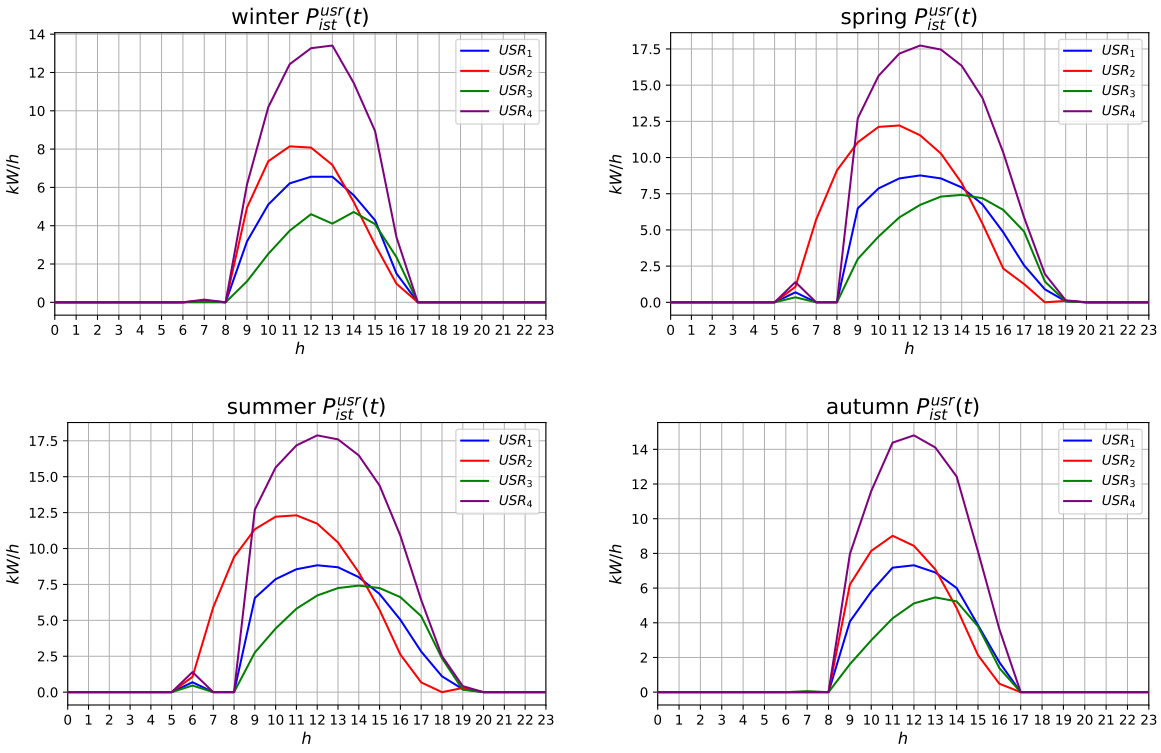

Figure 3.3: Amount of energy sent from each USR to IST.

Figure 3.4: IST and USRs' yearly savings as a function of the specific price of the installed equipment.

$\widehat{c}_{pv}$ [€ Wp^{-1}]	Savings [%]				
	IST	USR$_1$	USR$_2$	USR$_3$	USR$_4$
3.0	0.028	20.397	17.459	22.594	20.181
2.5	0.059	28.351	24.472	26.795	27.522
2.0	0.276	28.351	24.472	28.780	27.522
1.5	0.496	28.351	24.472	28.780	27.522
1.2	0.627	28.351	24.472	28.780	27.522
1.1	0.671	28.351	24.472	28.780	27.522
1.0	0.715	28.351	24.472	28.780	27.522

Table 3.2: Percentual savings obtained with the optimal solutions in the sensitivity analysis.

3.3 Sensitivity analysis

A sensitivity analysis has been performed by varying the price per PV module. The same has been done for the ST and TS systems, but these equipment are not part of the optimal solution even with a price of 200 € per collector and 500 € m^{-3} respectively. The thermal energy requirements do not justify the investment in ST under the model's assumptions.

The prices under analysis have been taken from [41]. In addition to that two more cases has been examined: those in which the specific costs are 2.5 and 3 € Wp^{-1}, for which the optimal configuration of PV modules are (42,59,31,85) and (20,11,17,42) respectively.

The sensitivity analysis presented in Tab. 3.2 shows that the price per watt-peak of a PV module affects principally the yearly savings of the campus, while those of the USRs remain unaffected when the number of modules installed do not change, as seen in Fig. 3.4. In the model the investment costs are entirely on IST, therefore USRs' savings are affected only when the cost per unit module is high enough that it is not convenient to exploit completely the available surface. The savings for IST are inversely proportional to the unitary cost of the PV modules, whereas for the USRs they are proportional to the available surfaces they can offer (assuming it being fully covered in PV modules).

3.4 Critical remarks

The system under analysis has been modeled under several simplifications and assumptions.

The design day technique is very useful because it reduces the complexity of the simulations (solving time), but it comes with the drawback of neglecting the positive and negative peaks in energy consumption and environmental conditions. Moreover, the design days are simulated independently: further studies should focus on the consequential simulation of time periods of at least a week long, to appreciate the variations from day to day and from weekdays to weekends.

Thermal loads are obtained from an approximation of the geometry of the residential complexes. This procedure can be performed with publicly available data and does not require to access technical maps, but its accuracy on the amount of electrical and thermal energy used might be insufficient for the actual design of the systems.

The advantages of the ST systems depend on both the correct characterization of the thermal loads and the accuracy of the model describing their behavior. Different results may be obtained with different modeling techniques – i.e. nonlinear programming – and iterative solution processes.

Further assessments should include the possibility to install micro and/or mini CHP or CCCHP systems in IST for the self production of electric, heating and cooling energy: these systems would work for many hours per year at rated load since IST base electricity consumption is about $800\,\mathrm{kW}$, and also the energy spent for HVAC during the day might justify cogenerative solutions.

IST makes profit by purchasing energy from the grid at night and selling it to the USRs at the same price they would normally buy it: this condition might not be acceptable for the grid management company, thus possibly undermining the feasibility of the project.

The last remark is that it has been assumed that the behavior of the residents does not change after the intervention: with the possibility of self-consuming the free renewable energy during the day, the electrical energy usage might increase. To avoid a decrease in residential energy efficiency as a consequence of the increase in renewable energy generation, compensating mechanisms and conditions should be investigated. For example, IST may demand a maximum (fixed or variable) share of renewable energy for the USR's self consumption, or a variable cost of the "discharged" energy according to the quantity it has received.

Chapter 4

Conclusions

This work presents an economic assessment of the design of a distributed PV system supplying with renewable electrical energy the residential complexes on which the equipment is installed and the university campus that finances the project. Four typical buildings have been studied to characterize the greatest number of residential complexes present locally. The campus was described by an electric consumption profile based on measured data. The geometry and occupancy of the residential complexes were estimated from publicly available data such as the number of floors, apartments per floor, and roof surface; according to these estimates an electric consumption profile obtained from measurements was associated to each apartment. Similarly, the thermal load for space heating was estimated with basis on the general thermal characteristics of the buildings and environmental recorded data, whereas that for domestic hot water was calculated as a function of the number of inhabitants. Two candidate technologies for energy generation were considered: photo-voltaic modules and solar thermal collectors with thermal storage. Both have been modeled with basis on environmental data (hourly solar radiation and external temperature) and technological parameters. From all the aforementioned data, four design days have been generated, each representative of a season of the year.

A MILP model was made to find the optimal configuration of the project, the objective function being the yearly energy-related costs.

The results show that the photo-voltaic is the only viable technology whereas the solar thermal equipments are never part of the optimal solutions. All of the roof surface is covered by modules, for a total of 221 modules at $580\,€$ each. IST, with an initial investment of $128\,180\,€$, benefits of a reduction of the yearly energy expenses of $0.276\,\%$ which equals to a profit of about $4684\,€$ per year, about $70\,k€$ at the end of the modules' lifetime (15 years). The highest share of savings is for the USRs, each of which saves between the $24.47\,\%$ and the $28.78\,\%$.

With this intervention the energy consumption of both the campus and the residents is reduced when the energy costs is at its highest. The campus also returns partially or completely the energy received when there is no renewable generation and the cost of energy is lower. The East-side surface orientation has shown to be preferable for it anticipates the renewable energy production covering the domestic peak load and allows the campus to receive more energy than the amount returned during the off-peak phase.

A sensitivity analysis on the unitary price of the technologies has been performed. The solar thermal technology is again never part of the optimal solutions, if the prices are lowered reasonably. The residential savings depend on the amount of installed modules, whereas the campus' depend on the specific cost of the technology. To higher specific prices of the PV modules correspond a decrease in the number of installed equipment, hence a reduction in economic benefits for both IST and the USRs; the least favorable examined scenario was with a unitary price of $3\,€\,\mathrm{Wp}^{-1}$, and under this conditions the total number of installed modules is 90. The yearly profit for IST is $0.028\,\%$, about $471\,€\,\mathrm{year}^{-1}$. The USRs savings decrease too, but the minimum one is still $17.5\,\%$. On the other hand, on the most favorable scenario, where the cost is $1\,€\,\mathrm{Wp}^{-1}$ the investment cost is only $64.09\,\mathrm{k}€$ and the yearly profit for IST is $0.715\,\%$, corresponding to $12.04\,\mathrm{k}€$, the USRs' savnings being the same as the base case.

The MILP model is simple and allows the assessment of many buildings one by one. The accuracy of the results can be enhanced with an improved characterization of the residential complexes and their energy flows, and an analysis based on extended real time periods. Smart procedures, conditions, and constraints should be investigated in future works to avoid the development of energy inefficient practices as a result of the availability of free renewable energy.

Bibliography

[1] European Commission. 2020 climate & energy package. https://ec.europa.eu/clima/policies/strategies/2020_en#tab-0-0. Accessed: 2018-10-08.

[2] European Commission. *Energy roadmap 2050*. Publications Office of the Europan Union, 2012.

[3] United Nations. *World Urbanization Prospects*. New York, 2014.

[4] European Commission. Communication from the commission to the european parliament, the council, the european economic and social committee and the committee of the regions. http://ww.w.xploit-eu.com/pdfs/Europe%202020%20Flagship%20Initiative%20INNOVATION.pdf, 2010. Accessed: 2018-10-01.

[5] European Environment Agency. Overall progress towards the european union's '20-20-20' climate and energy targets. https://web.archive.org/web/20181001164223/https://www.eea.europa.eu/themes/climate/trends-and-projections-in-europe/trends-and-projections-in-europe-2017/overall-progress-towards-the-european. Accessed: 2018-10-01.

[6] Diário da Républica. Regulamento das Características de Comportamento Térmico dos Edifícios (RCCTE), Decreto-Lei n.o 80/2006. *Diário da República - I Série - A - n°67*, pages 46(2468–2513), 2006.

[7] Diário da Républica. Regulamento de Desempenho Energético dos Edifícios de Habitação (REH), Decreto-Lei n.o 118/2013. *Diário da República - I Série - A*, pages 46(2468–2513), 2013.

[8] International Energy Agency. *Renewables Information 2018*. OECD, 2018. doi: 10.1787/renew-2018-en. URL https://doi.org/10.1787/renew-2018-en.

[9] European Commission Photovoltaic Geographical Information System. Global irradiation and solar electricity potential. http://re.jrc.ec.europa.eu/pvg_download/map_index.html#! Accessed: 2018-10-01.

[10] G. Chicco and P. Mancarella. Distributed multi-generation: A comprehensive view. *Renewable and Sustainable Energy Reviews*, 13(3):535–551, apr 2009. doi: 10.1016/j.rser.2007.11.014. URL https://doi.org/10.1016/j.rser.2007.11.014.

[11] M. Mohammadi, Y. Noorollahi, B. Mohammadi-ivatloo, and H. Yousefi. Energy hub: From a model to a concept – a review. *Renewable and Sustainable Energy Reviews*, 80:1512–1527, dec 2017. doi: 10.1016/j.rser.2017.07.030. URL https://doi.org/10.1016/j.rser.2017.07.030.

[12] A. Alarcon-Rodriguez, G. Ault, and S. Galloway. Multi-objective planning of distributed energy resources: A review of the state-of-the-art. *Renewable and Sustainable Energy Reviews*, 14(5): 1353–1366, jun 2010. doi: 10.1016/j.rser.2010.01.006. URL https://doi.org/10.1016/j.rser.2010.01.006.

[13] M. Sameti and F. Haghighat. Optimization approaches in district heating and cooling thermal network. *Energy and Buildings*, 140:121–130, apr 2017. doi: 10.1016/j.enbuild.2017.01.062. URL https://doi.org/10.1016/j.enbuild.2017.01.062.

[14] K. Orehounig, R. Evins, and V. Dorer. Integration of decentralized energy systems in neighbourhoods using the energy hub approach. *Applied Energy*, 154:277–289, sep 2015. doi: 10.1016/j.apenergy.2015.04.114. URL https://doi.org/10.1016/j.apenergy.2015.04.114.

[15] S. G. Sigarchian, A. Malmquist, and V. Martin. The choice of operating strategy for a complex polygeneration system: A case study for a residential building in italy. *Energy Conversion and Management*, 163:278–291, may 2018. doi: 10.1016/j.enconman.2018.02.066. URL https://doi.org/10.1016/j.enconman.2018.02.066.

[16] A. Fetanat and E. Khorasaninejad. Size optimization for hybrid photovoltaic–wind energy system using ant colony optimization for continuous domains based integer programming. *Applied Soft Computing*, 31:196–209, jun 2015. doi: 10.1016/j.asoc.2015.02.047. URL https://doi.org/10.1016/j.asoc.2015.02.047.

[17] A. Christidis, C. Koch, L. Pottel, and G. Tsatsaronis. The contribution of heat storage to the profitable operation of combined heat and power plants in liberalized electricity markets. *Energy*, 41(1):75–82, may 2012. doi: 10.1016/j.energy.2011.06.048. URL https://doi.org/10.1016/j.energy.2011.06.048.

[18] S. Rech and A. Lazzaretto. Smart rules and thermal, electric and hydro storages for the optimum operation of a renewable energy system. *Energy*, 147:742–756, mar 2018. doi: 10.1016/j.energy.2018.01.079. URL https://doi.org/10.1016/j.energy.2018.01.079.

[19] H. Ren and W. Gao. A MILP model for integrated plan and evaluation of distributed energy systems. *Applied Energy*, 87(3):1001–1014, mar 2010. doi: 10.1016/j.apenergy.2009.09.023. URL https://doi.org/10.1016/j.apenergy.2009.09.023.

[20] A. Costa and A. Fichera. A mixed-integer linear programming (MILP) model for the evaluation of CHP system in the context of hospital structures. *Applied Thermal Engineering*, 71(2):921–929, oct 2014. doi: 10.1016/j.applthermaleng.2014.02.051. URL https://doi.org/10.1016/j.applthermaleng.2014.02.051.

[21] M. Ameri and Z. Besharati. Optimal design and operation of district heating and cooling networks with CCHP systems in a residential complex. *Energy and Buildings*, 110:135–148, jan 2016. doi: 10.1016/j.enbuild.2015.10.050. URL https://doi.org/10.1016/j.enbuild.2015.10.050.

[22] L. A. Wolsey. *Integer Programming*. Wiley, 1 edition, 1998. ISBN 9780471283669.

[23] A. Omu, S. Hsieh, and K. Orehounig. Mixed integer linear programming for the design of solar thermal energy systems with short-term storage. *Applied Energy*, 180:313–326, oct 2016. doi: 10.1016/j.apenergy.2016.07.055. URL https://doi.org/10.1016/j.apenergy.2016.07.055.

[24] Berkeley Lab. Distributed energy resources - customer adoption model. https://building-microgrid.lbl.gov/projects/der-cam. Accessed: 2018-10-03.

[25] J. Jung and M. Villaran. Optimal planning and design of hybrid renewable energy systems for microgrids. *Renewable and Sustainable Energy Reviews*, 75:180–191, aug 2017. doi: 10.1016/j.rser.2016.10.061. URL https://doi.org/10.1016/j.rser.2016.10.061.

[26] J. H. Braslavsky, J. R. Wall, and L. J. Reedman. Optimal distributed energy resources and the cost of reduced greenhouse gas emissions in a large retail shopping centre. *Applied Energy*, 155:120–130, oct 2015. doi: 10.1016/j.apenergy.2015.05.085. URL https://doi.org/10.1016/j.apenergy.2015.05.085.

[27] M. Stadler, M. Groissböck, G. Cardoso, and C. Marnay. Optimizing distributed energy resources and building retrofits with the strategic DER-CAModel. *Applied Energy*, 132:557–567, nov 2014. doi: 10.1016/j.apenergy.2014.07.041. URL https://doi.org/10.1016/j.apenergy.2014.07.041.

[28] GAMS Software GmbH. An introduction to gams. https://www.gams.com/products/introduction/. Accessed: 2018-10-03.

[29] IBM. IBM ILOG CPLEX Optimization Studio CPLEX User's Manual. https://www.ibm.com/support/knowledgecenter/SSSA5P_12.8.0/ilog.odms.studio.help/pdf/usrcplex.pdf?origURL=SSSA5P_12.8.0/ilog.odms.studio.help/Optimization_Studio/topics/PLUGINS_ROOT/ilog.odms.studio.help/pdf/usrcplex.pdf. Accessed: 2018-10-03.

[30] Gurobi Optimization, LLC. Gurobi optimizer reference manual. http://www.gurobi.com/documentation/8.0/refman/index.html. Accessed: 2018-10-03.

[31] P. Gabrielli, M. Gazzani, E. Martelli, and M. Mazzotti. Optimal design of multi-energy systems with seasonal storage. *Applied Energy*, 219:408–424, jun 2018. doi: 10.1016/j.apenergy.2017.07.142. URL https://doi.org/10.1016/j.apenergy.2017.07.142.

[32] Instituto Superior Técnico. Campus sustentável. http://sustentavel.unidades.tecnico.ulisboa.pt/. Accessed: 2018-10-04.

[33] A. S. Stavropoulos. Spatial analysis of heating and cooling energy needs in lisbon. Master's thesis, Instituto Superior Técnico, 2013.

[34] Municípia and Lisboa E-Nova. Carta de potencial solar. http://80.251.174.200/lisboae-nova/potencialsolar/. Accessed: 2018-10-05.

[35] Instituto Nacional de Estatística. Censos 2001 - importação dos principais dados alfanuméricos e geográficos (BGRI). http://mapas.ine.pt/download/index2001.phtml. Accessed: 2018-10-05.

[36] ADENE. Medidas ppec 2013-2014. https://www.adene.pt/comportamentos/medidas-ppec-2013-2014/. Accessed: 2018-10-05.

[37] S. M. Magalhães and V. M. Leal. Characterization of thermal performance and nominal heating gap of the residential building stock using the EPBD-derived databases: The case of portugal mainland. *Energy and Buildings*, 70:167–179, feb 2014. doi: 10.1016/j.enbuild.2013.11.054. URL https://doi.org/10.1016/j.enbuild.2013.11.054.

[38] A. Durmayaz, M. Kadıoğlu, and Z. Şen. An application of the degree-hours method to estimate the residential heating energy requirement and fuel consumption in istanbul. *Energy*, 25(12):1245–1256, dec 2000. doi: 10.1016/s0360-5442(00)00040-2. URL https://doi.org/10.1016/s0360-5442(00)00040-2.

[39] A. D. S. Santos. Avaliação de sistemas solares térmicos de produção de Água quente sanitária em edifícios de habitação multifamiliar. Master's thesis, Instituto Superior Técnico, 2012.

[40] Sunmodule Plus. Sw 290 mono (5-busbar) photovoltaic module. https://web.archive.org/web/20181014162534/https://www.solarelectricsupply.com/solar-panels/solar-world/solarworld-sunmodule-plus-sw-300-watt-mono-five-busbar-solar-panel-wholesale. Accessed: 2018-10-01.

[41] C. H. Villar, D. Neves, and C. A. Silva. Solar PV self-consumption: An analysis of influencing indicators in the portuguese context. *Energy Strategy Reviews*, 18:224–234, dec 2017. doi: 10.1016/j.esr.2017.10.001. URL https://doi.org/10.1016/j.esr.2017.10.001.

[42] J. A. Duffie and W. A. Beckman. *Solar engineering of thermal processes*. John Wiley & Sons, 2013.

[43] B. Y. Liu and R. C. Jordan. The long-term average performance of flat-plate solar-energy collectors. *Solar Energy*, 7(2):53–74, apr 1963. doi: 10.1016/0038-092x(63)90006-9. URL https://doi.org/10.1016/0038-092x(63)90006-9.

[44] W. Durisch, B. Bitnar, J.-C. Mayor, H. Kiess, K. hang Lam, and J. Close. Efficiency model for photovoltaic modules and demonstration of its application to energy yield estimation. *Solar Energy Materials and Solar Cells*, 91(1):79–84, jan 2007. doi: 10.1016/j.solmat.2006.05.011. URL https://doi.org/10.1016/j.solmat.2006.05.011.

Appendix A

Model of the solar energy production

This chapter presents the process performed to obtain the electrical and thermal output energy for a PV module and ST collector respectively. The calculations, as well as the nomenclature, are the same as [42].

The inputs are hourly median hourly values for solar radiation and temperature, obtained with the same process presented in 2.1.3, and the constants shown in Table A.1. The angles presented in the table are expressed in degrees for clarity. In the calculations they are converted into radians. It is assumed that the modules will be oriented according to the normal to the façade of the building they will be installed on, therefore each USR will have a different specific solar energy production profile. All the angles used in the calculations are converted into radians.

Geographic		Geometric		Others	
ϕ	38.7 deg N	β	38.7 deg	G_{sc}	1367 W m^{-2}
Lat	9 deg W	γ	$\gamma_u \forall u \in U$	ρ_g	0.2
h	70 m				

Table A.1: Constants used to model the incident solar radiation on a sloped surface.

A.1 Incident solar radiation on a surface

$$B = (n-1) \cdot \frac{360}{365} \tag{A.1}$$

$$\begin{aligned} G_{on} = G_{sc} \cdot [&1.000\,110 + 0.034\,221 \cdot \cos B + 0.001\,280 \cdot \sin B \\ &+ 0.000\,719 \cdot \cos(2B) + 0.000\,077 \cdot \sin(2B)] \end{aligned} \tag{A.2}$$

$$\begin{aligned} E = 2.292 \cdot (&0.0075 + 0.1868 \cdot \cos B - 3.2077 \cdot \sin B \\ &- 1.4615 \cdot \cos(2B) - 4.089 \cdot \sin(2B)) \end{aligned} \tag{A.3}$$

$$t_{sol} = \frac{h \cdot 60 + E - 4 \cdot Lat}{60} \tag{A.4}$$

$$\omega = \text{rad}(15 \cdot t_{sol} - 180) \tag{A.5}$$

$$\begin{aligned} \delta = &0.006\,918 - 0.399\,912 \cdot \cos B + 0.070\,257 \cdot \sin B \\ &- 0.006\,758 \cdot \cos(2B) + 0.000\,907 \cdot \sin(2B) 0.002\,697 \cdot \cos(3B) \\ &0.001\,48 \cdot \sin(3B) \end{aligned} \tag{A.6}$$

$$\omega_{sc} = \arccos(-\tan\delta \cdot \tan(\phi)) \tag{A.7}$$

$$\omega_{ss,\text{surf.}} = \arccos(-\tan\delta \cdot \tan(\phi - \beta)) \tag{A.8}$$

$$\omega_{ss} = \min\{\omega_{sc}, \omega_{ss,\text{surf.}}\} \tag{A.9}$$

$$\omega_{sr} = -\omega_{ss}. \tag{A.10}$$

All the calculations revolve around solar time, and the daylight saving time (DST) has not been taken into account. As shown in Eq. (A.4) the relation between standard time (h) and solar time (t_{sol}) is linear: an hour difference in standard time corresponds to the same difference in solar time. The solar hour angle (ω) is negative before the *solar midday* (the sun is at the zenit), and later it assumes positive values. Equations (A.7) and (A.8) calculate the sunset solar angle hour. A sloped surface can be shaded by the actual sunset or by itself: the *real* sunset hour (ω_{ss}) is the minimum between the solar(ω_{sc}) and the surface ($\omega_{ss,\text{surf.}}$) sunset hour angles, as imposed by (A.9). Thanks to the symmetry ensured by working with solar time, the sunrise hour (ω_{sr}) is equal and opposite of the sunset one.

The incident angle (θ) the sun has with a tilted surface is calculated with:

$$\begin{aligned} \cos\theta = &\sin\delta\sin\phi\cos\beta - \sin\delta\cos\phi\sin\beta\cos\gamma + \cos\delta\cos\phi\cos\beta\cos\omega_m \\ &+ \cos\delta\sin\phi\sin\beta\cos\gamma\cos\omega_m + \cos\delta\sin\beta\sin\gamma\sin\omega_m, \end{aligned} \tag{A.11}$$

being ω_m the midpoint between two subsequent hour angles:

$$\omega_m = \frac{\omega_1 + \omega_2}{2}. \tag{A.12}$$

If between an interval sunrise or sunset occur, the following algorithm ensures that the sunrise/sunset hour becomes one of the extremes (assuming ω_2 always follows ω_1):

$$
\begin{aligned}
&if && \omega_h < \omega_{sr} \quad and \quad \omega_{h+1} > \omega_{sr}: \\
&&& \omega_1 = \omega_{sr} \\
&&& \omega_2 = \omega_{h+1} \\
&elseif && \omega_h < \omega_{ss} \quad and \quad \omega_{h+1} > \omega_{ss}: \\
&&& \omega_1 = \omega_h \\
&&& \omega_2 = \omega_{ss} \\
&else: && \omega_1 = \omega_h \\
&&& \omega_2 = \omega_{h+1}.
\end{aligned}
$$

The measured irradiance and the extraterrestrial irradiance on an horizontal surface, between sunrise and sunset, can be calculated as

$$I = G \cdot \left(\frac{\deg(\omega_2 - \omega_1)}{15 \cdot 3600} \right) \left[\mathrm{J\,m^{-2}} \right] \tag{A.13}$$

$$I_0 = \frac{24 \cdot 3600}{2\pi} G_{on} \cdot (\cos\phi \cos\delta (\sin\omega_2 - \sin\omega_1) + (\omega_2 - \omega_1) \sin\phi \sin\delta) \left[\mathrm{J\,m^{-2}} \right]. \tag{A.14}$$

The isotropic sky model has been chosen for modeling the incident radiation on a sloped surface, due to its simplicity and effectiveness [43]. The model relies on the assumption that the radiation is made of three components: beam, isotropic diffuse, and diffused ground-reflected radiation. The total solar radiation on a tilted surface for an hour is the sum of the tree terms:

$$I_T = I_b R_b + I_d \left(\frac{1 + \cos\beta}{2} \right) + I\rho_g \left(\frac{1 - \cos\beta}{2} \right) \quad \left[\mathrm{J\,m^{-2}} \right]. \tag{A.15}$$

R_b is the ratio of beam radiation on the plane to that on an horizontal surface:

$$R_b = \frac{\cos\theta}{\cos\theta_z}, \tag{A.16}$$

where:

$$cos\theta_z = \cos\delta \cos\omega_m \cos\phi + \sin\delta \sin\phi. \tag{A.17}$$

In some days the sunset/sunrise occurs closely enough to the beginning of the following, thus resulting in very low values of $\cos\theta_z$. The ratio has therefore been limited to a maximum value of 30, in order not to have impossible values of the beam radiation.

I_d is the isotropic diffuse radiation, which is found by the following correlation:

$$\frac{I_d}{I} = \begin{cases} 1.0 - 0.09k_T & \text{for } k_T \leq 0.22 \\ 0.9511 - 0.1604k_T + 4.388k_T^2 & \text{for } 0.22 < k_T \leq 0.8 \\ \qquad -16.638k_T^2 + 12.336k_T^4 & \\ 0.165 & \text{for } k_T > 0.8, \end{cases} \tag{A.18}$$

where k_T is the clearness index, defined as:

$$k_t = \frac{I}{I_0}. \tag{A.19}$$

Again, for short time-spans, values of k_T higher than 1 can be obtained. This is impossible, because it would mean that the total radiation arriving on the Earth's surface (I) is greater than the total extraterrestrial radiation (I_0), which is impossible and is a consequence of working with small time intervals, therefore all the values have been rounded down to 1 when necessary.

Eventually the total radiation incident on a tilted surface is obtained with:

$$G_T = I_T \cdot \left(\frac{15 \cdot 3600}{\deg(\omega_2 - \omega_1)} \right) \left[\mathrm{W\,m^{-2}} \right]. \tag{A.20}$$

A.2 PV energy production

The selected PV technology is a mono crystalline silicium (mono-SI) panel manufactured by [40]. Its characteristic curves are presented in Fig. A.1.

The power output of a PV module is modeled as a function of the incident solar radiation and the ambient temperature as proposed by Durisch et al. [44].

The efficiency is:

$$\eta_{pv} = p \cdot \left[q \frac{G_T}{G_{T,ref}} + \left(\frac{G_T}{G_{T,ref}} \right)^m \right] \cdot \left[1 + r \frac{T_M}{T_{M,ref}} + s \frac{am}{am_r ef} + \left(\frac{G_T}{G_{T,ref}} \right)^u \right], \tag{A.21}$$

where $G_{T,ref} = 1000\,\mathrm{W\,m^{-2}}$ is the reference solar radiation, $T_{M,ref} = 25\,^\circ\mathrm{C}$ is the reference module temperature and $m_0 = 1.5$ the reference air mass. The coefficients p, q, r, s, u for mono-Si modules are equal to 0.2362, 0.2983, 0.9795 and 0.9865 respectively.

The air mass is calculated as:

$$am = \frac{\exp\left(-0.0001184h\right)}{\cos\theta_z + 0.5057(96.08 - \deg(\theta_z))^{-1.634}}, \tag{A.22}$$

while the module temperature as:

$$T_M = T_{amb} + h \cdot G_T, \tag{A.23}$$

where h for mono-SI modules is equal to 0.028. All the temperatures are expressed in °C. The direct

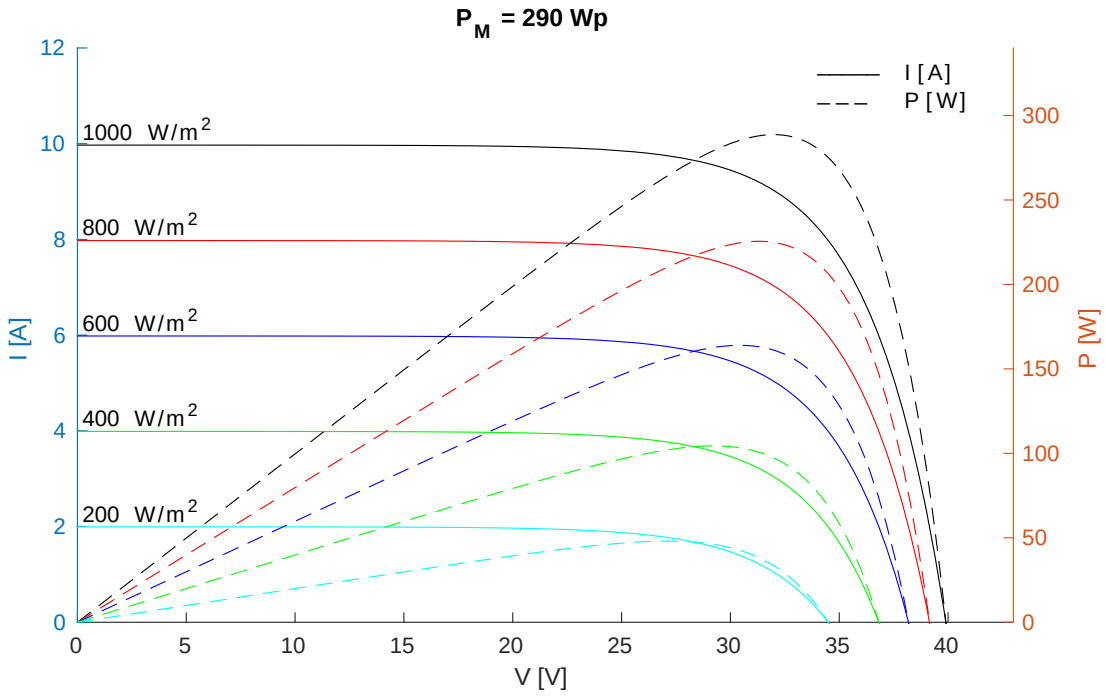

Figure A.1: Characteristic curves of the PV modules.

current (DC) power output of a PV module is eventually calculated as:

$$p_{pv} = G_T \cdot A_{mod} \cdot \eta_{el,mod} \cdot \frac{1\,\mathrm{W}}{1000\,\mathrm{kW}}[\mathrm{kW}], \tag{A.24}$$

with $A_{mod} = 1.677\,\mathrm{m}^2$.

The total output power of the installation is the algebraic sum of the output powers of the single modules. The inverter efficiency is assumed to be equal to $98\,\%$.

A.3 ST energy production

The solar thermal energy output does not only depend on the physical properties of the collector itself, but also on the inlet fluid temperature. This changes accordingly with the temperature inside the TS (which depends on the tank capacity and the energy subtraction from the users).

The heat generated by a collector, Q_u, is:

$$Q_u = \dot{m}_f c_p (T_{f,o} - T_{f,i}) = A_{coll}[G_T(\tau\alpha) - (T_{f,i} - T_{amb})], \tag{A.25}$$

where $\dot{m}_f$ is the water-glycole flow rate, c_p its specific heat, $T_{f,o}$ and $T_{f,i}$ the outlet and inlet temperatures of the fluid.

To keep the model simple and independent from the storage tank capacity (which is a decision variable of the optimization problem), the collector inlet temperature has been fixed at $60\,^{\circ}\mathrm{C}$. This is the minimum temperature allowed for the storage of hot water to avoid proliferation of pathogens.

Eventually, the specific

$$q_{st} = A_{coll}(F_R(\tau\alpha)G_T - F_R U_L(T_{f,i} - T_{amb}))\frac{1\,\text{W}}{1000\,\text{kW}}[\text{kW}], \tag{A.26}$$

being F_R the heat removal factor, and U_L the overall heat loss coefficient. A typical solar flat plate collector has a $F_R(\tau\alpha)$ of 0.68 and $F_R U_L$ of 4.9 [23].

A.4 Final parameters handling

Following the aforementioned processes, an electrical and thermal energy output (in kWh) have been associated to each hour of the year. From this, four design days were obtained through the same process shown in Fig. 2.4.